Health, Labor and Welfare of Japan, from the Ministry of Education, Culture, Sports, Science and Technology, by the Research on Health Sciences Focusing on Drug Innovation from the Japan Health Sciences Foundation, and by the National Institute of Biomedical Innovation.

Appendix A. Supplementary data

Supplementary data associated with this article can be found, in the online version, at doi:10.1016/j.bbrc.2011.05.144.

References

[1] T. Wakita, T. Pietschmann, T. Kato, T. Date, M. Miyamoto, Z. Zhao, K. Murthy, A. Habermann, H.G. Krausslich, M. Mizokami, R. Bartenschlager, T.J. Liang, Production of infectious hepatitis C virus in tissue culture from a cloned viral genome, Nat. Med. 11 (2005) 791–796.

[2] M. Yi, R.A. Villanueva, D.L. Thomas, T. Wakita, S.M. Lemon, Production of infectious genotype 1a hepatitis C virus (Hutchinson strain) in cultured human hepatoma cells, Proc. Natl. Acad. Sci. USA 103 (2006) 2310–2315.

[3] M.J. Evans, C.M. Rice, S.P. Goff, Phosphorylation of hepatitis C virus nonstructural protein 5A modulates its protein interactions and viral RNA replication, Proc. Natl. Acad. Sci. USA 101 (2004) 13038–13043.

[4] N. Appel, M. Zayas, S. Miller, J. Krijnse-Locker, T. Schaller, P. Friebe, S. Kallis, U. Engel, R. Bartenschlager, Essential role of domain III of nonstructural protein 5A for hepatitis C virus infectious particle assembly, PLoS Pathog. 4 (2008) e1000035.

[5] N. Appel, U. Herian, R. Bartenschlager, Efficient rescue of hepatitis C virus RNA replication by trans-complementation with nonstructural protein 5A, J. Virol. 79 (2005) 896–909.

[6] M. Yanagi, R.H. Purcell, S.U. Emerson, J. Bukh, Transcripts from a single full-length cDNA clone of hepatitis C virus are infectious when directly transfected into the liver of a chimpanzee, Proc. Natl. Acad. Sci. USA 94 (1997) 8738–8743.

[7] V. Lohmann, F. Korner, J. Koch, U. Herian, L. Theilmann, R. Bartenschlager, Replication of subgenomic hepatitis C virus RNAs in a hepatoma cell line, Science 285 (1999) 110–113.

[8] M. Yanagi, R.H. Purcell, S.U. Emerson, J. Bukh, Hepatitis C virus: an infectious molecular clone of a second major genotype (2a) and lack of viability of intertypic 1a and 2a chimeras, Virology 262 (1999) 250–263.

[9] K. Murakami, M. Abe, T. Kageyama, N. Kamoshita, A. Nomoto, Down-regulation of translation driven by hepatitis C virus internal ribosomal entry site by the 3′ untranslated region of RNA, Arch. Virol. 146 (2001) 729–741.

[10] J. Zhong, P. Gastaminza, G. Cheng, S. Kapadia, T. Kato, D.R. Burton, S.F. Wieland, S.L. Uprichard, T. Wakita, F.V. Chisari, Robust hepatitis C virus infection in vitro, Proc. Natl. Acad. Sci. USA 102 (2005) 9294–9299.

[11] D. Akazawa, T. Date, K. Morikawa, A. Murayama, M. Miyamoto, M. Kaga, H. Barth, T.F. Baumert, J. Dubuisson, T. Wakita, CD81 expression is important for the permissiveness of Huh7 cell clones for heterogeneous hepatitis C virus infection, J. Virol. 81 (2007) 5036–5045.

[12] M. Gao, R.E. Nettles, M. Belema, L.B. Snyder, V.N. Nguyen, R.A. Fridell, M.H. Serrano-Wu, D.R. Langley, J.H. Sun, D.R. O'Boyle 2nd, J.A. Lemm, C. Wang, J.O. Knipe, C. Chien, R.J. Colonno, D.M. Grasela, N.A. Meanwell, L.G. Hamann, Chemical genetics strategy identifies an HCV NS5A inhibitor with a potent clinical effect, Nature 465 (2010) 96–100.

[13] T. Kato, Y. Choi, G. Elmowalid, R.K. Sapp, H. Barth, A. Furusaka, S. Mishiro, T. Wakita, K. Krawczynski, T.J. Liang, Hepatitis C virus JFH-1 strain infection in chimpanzees is associated with low pathogenicity and emergence of an adaptive mutation, Hepatology 48 (2008) 732–740.

[14] A. Kaul, S. Stauffer, C. Berger, T. Pertel, J. Schmitt, S. Kallis, M. Zayas, V. Lohmann, J. Luban, R. Bartenschlager, Essential role of cyclophilin A for hepatitis C virus replication and virus production and possible link to polyprotein cleavage kinetics, PLoS Pathog. 5 (2009) e1000546.

[15] R. Bartenschlager, L. Ahlborn-Laake, K. Yasargil, J. Mous, H. Jacobsen, Substrate determinants for cleavage in cis and in trans by the hepatitis C virus NS3 proteinase, J. Virol. 69 (1995) 198–205.

[16] A. Urbani, E. Bianchi, F. Narjes, A. Tramontano, R. De Francesco, C. Steinkuhler, A. Pessi, Substrate specificity of the hepatitis C virus serine protease NS3, J. Biol. Chem. 272 (1997) 9204–9209.

[17] T. Masaki, R. Suzuki, K. Murakami, H. Aizaki, K. Ishii, A. Murayama, T. Date, Y. Matsuura, T. Miyamura, T. Wakita, T. Suzuki, Interaction of hepatitis C virus nonstructural protein 5A with core protein is critical for the production of infectious virus particles, J. Virol. 82 (2008) 7964–7976.

[18] W. Cun, J. Jiang, G. Luo, The C-terminal alpha-helix domain of apolipoprotein E is required for interaction with nonstructural protein 5A and assembly of hepatitis C virus, J. Virol. 84 (2010) 11532–11541.

[19] J.A. Lemm, D. O'Boyle 2nd, M. Liu, P.T. Nower, R. Colonno, M.S. Deshpande, L.B. Snyder, S.W. Martin, D.R. St Laurent, M.H. Serrano-Wu, J.L. Romine, N.A. Meanwell, M. Gao, Identification of hepatitis C virus NS5A inhibitors, J. Virol. 84 (2010) 482–491.

[20] T.K. Scheel, J.M. Gottwein, L.S. Mikkelsen, T.B. Jensen, J. Bukh, Recombinant HCV variants with NS5A from genotypes 1–7 have different sensitivities to an NS5A inhibitor but not interferon-alpha, Gastroenterology 140 (2011) 1032–1042.

[21] R.A. Fridell, D. Qiu, C. Wang, L. Valera, M. Gao, Resistance analysis of the hepatitis C virus NS5A inhibitor BMS-790052 in an in vitro replicon system, Antimicrob. Agents Chemother. 54 (2010) 3641–3650.

[22] K. Yoshioka, S. Kakumu, T. Wakita, T. Ishikawa, Y. Itoh, M. Takayanagi, Y. Higashi, M. Shibata, T. Morishima, Detection of hepatitis C virus by polymerase chain reaction and response to interferon-alpha therapy: relationship to genotypes of hepatitis C virus, Hepatology 16 (1992) 293–299.

JVI
Journals.ASM.org

Production of Infectious Chimeric Hepatitis C Virus Genotype 2b Harboring Minimal Regions of JFH-1

Asako Murayama,[a] Takanobu Kato,[a] Daisuke Akazawa,[a] Nao Sugiyama,[a] Tomoko Date,[a] Takahiro Masaki,[a] Shingo Nakamoto,[b] Yasuhito Tanaka,[c] Masashi Mizokami,[d] Osamu Yokosuka,[b] Akio Nomoto,[e]* and Takaji Wakita[a]

Department of Virology II, National Institute of Infectious Diseases, Shinjuku-ku, Tokyo, Japan[a]; Department of Medicine and Clinical Oncology, Graduate School of Medicine, Chiba University, Chuo, Chiba, Japan[b]; Department of Virology and Liver Unit, Nagoya City University Graduate School of Medical Sciences, Kawasumi, Mizuho, Nagoya, Japan[c]; The Research Center for Hepatitis and Immunology, National Center for Global Health and Medicine, Ichikawa, Chiba, Japan[d]; and Department of Microbiology, Graduate School of Medicine, University of Tokyo, Bunkyo-ku, Tokyo, Japan[e]

To establish a cell culture system for chimeric hepatitis C virus (HCV) genotype 2b, we prepared a chimeric construct harboring the 5′ untranslated region (UTR) to the E2 region of the MA strain (genotype 2b) and the region of p7 to the 3′ UTR of the JFH-1 strain (genotype 2a). This chimeric RNA (MA/JFH-1.1) replicated and produced infectious virus in Huh7.5.1 cells. Replacement of the 5′ UTR of this chimera with that from JFH-1 (MA/JFH-1.2) enhanced virus production, but infectivity remained low. In a long-term follow-up study, we identified a cell culture-adaptive mutation in the core region (R167G) and found that it enhanced virus assembly. We previously reported that the NS3 helicase (N3H) and the region of NS5B to 3′ X (N5BX) of JFH-1 enabled replication of the J6CF strain (genotype 2a), which could not replicate in cells. To reduce JFH-1 content in MA/JFH-1.2, we produced a chimeric viral genome for MA harboring the N3H and N5BX regions of JFH-1, combined with a JFH-1 5′ UTR replacement and the R167G mutation (MA/N3H+N5BX-JFH1/R167G). This chimeric RNA replicated efficiently, but virus production was low. After the introduction of four additional cell culture-adaptive mutations, MA/N3H+N5BX-JFH1/5am produced infectious virus efficiently. Using this chimeric virus harboring minimal regions of JFH-1, we analyzed interferon sensitivity and found that this chimeric virus was more sensitive to interferon than JFH-1 and another chimeric virus containing more regions from JFH-1 (MA/JFH-1.2/R167G). In conclusion, we established an HCV genotype 2b cell culture system using a chimeric genome harboring minimal regions of JFH-1. This cell culture system may be useful for characterizing genotype 2b viruses and developing antiviral strategies.

Hepatitis C virus (HCV) is a major cause of chronic liver disease (5, 13), but the lack of a robust cell culture system to produce virus particles has hampered the progress of HCV research (2). Although the development of a subgenomic replicon system has enabled research into HCV RNA replication (15), infectious virus particle production has not been possible. Recently, an HCV cell culture system was developed using a genotype 2a strain, JFH-1, cloned from a fulminant hepatitis patient (14, 29, 32), thereby allowing investigation of the entire life cycle of this virus. However, several groups of investigators have reported genotype- and/or strain-dependent effects of some antiviral reagents (6, 17) and neutralizing antibodies (7, 25). Therefore, efficient virus production systems using various genotypes and strains are indispensable for HCV research and the development of antiviral strategies.

The JFH-1 strain is the first HCV strain that can efficiently produce HCV particles in HuH-7 cells (29). Other strains can replicate and produce infectious virus by HCV RNA transfection, but the efficiency is far lower than that of JFH-1 (24, 31). In the case of replication-incompetent strains, chimeric virus containing the JFH-1 nonstructural protein coding region is useful for analyses of viral characteristics (6, 9, 14, 23, 30, 31).

In this study, we developed a genotype 2b chimeric infectious virus production system using the MA strain (accession number AB030907) (19) harboring minimal regions of JFH-1 and cell culture-adaptive mutations that enhance infectious virus production.

MATERIALS AND METHODS

Cell culture. Huh7.5.1 cells (a kind gift from Francis V. Chisari) (32) and Huh7-25 cells (1) were cultured at 37°C in Dulbecco's modified Eagle's medium containing 10% fetal bovine serum under 5% CO_2 conditions. For follow-up study, RNA-transfected cells were passaged every 2 to 5 days depending on cell status.

Full-length genomic HCV constructs. Plasmids used in the analysis of genomic RNA replication were constructed based on pJFH1 (29) and pMA (19). For convenience, an EcoRI recognition site was introduced upstream of the T7 promoter region of pMA by PCR, and an XbaI recognition site was introduced at the end of the 3′ untranslated region (UTR). To construct MA/JFH-1, the EcoRI-BsaBI (nucleotides [nt] 1 to 2570; 5′ UTR to E2) fragment of pMA was substituted into pJFH1 (Fig. 1A). Replacement of the 5′ UTR was performed by exchanging the EcoRI-AgeI (nt 1 to 159) fragment. A point mutation in the core region (R167G) was introduced into MA chimeric constructs by PCR using the following primers: sense, 5′-TTA TGC AAC GGG GAA TTT ACC CGG TTG CTC T-3′; antisense, 5′-GGT AAA TTC CCC GTT GCA TAA TTT ATC CCG TC-3′. G167R substitution in the JFH-1 construct was performed by PCR using the following primers: sense, 5′-ATT ATG CAA CAA GGA ACC TAC CCG GTT TCC C-3′; antisense, 5′-GGT AGG TTC CTT GTT GCA TAA TTA ACC CCG TC-3′. Point mutations (L814S, R1012G, T1106A, and V1951A) were introduced into MA chimeric constructs by PCR using the following primers: L814S, 5′-GCT TAC GCC TCG GAC GCC GCT GAA CAA GGG G-3′ (sense) and 5′-AGC GGC GTC CGA GGC GTA AGC CTG CTG CGG C-3′ (antisense); R1012G, 5′-GAG GCT AGG TGG

Received 13 June 2011 Accepted 23 November 2011
Published ahead of print 7 December 2011
Address correspondence to Takaji Wakita, wakita@nih.go.jp.
* Present address: Institute of Microbial Chemistry, Shinagawa-ku, Tokyo, Japan.

doi:10.1128/JVI.05386-11

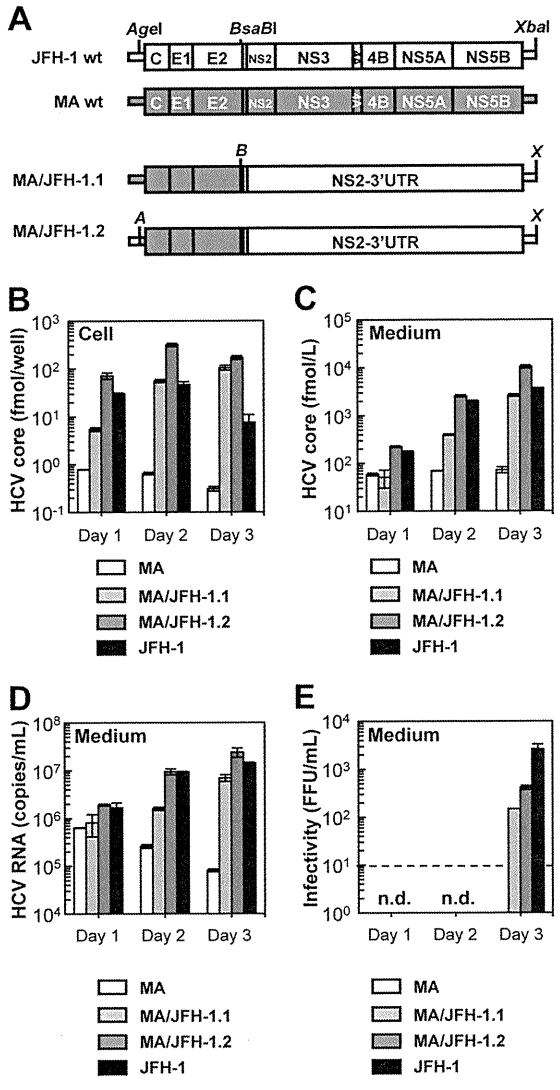

FIG 1 Replication and virus production by MA/JFH-1 chimeras in Huh7.5.1 cells. (A) Schematic structures of JFH-1, MA, and two MA/JFH-1 chimeras (MA/JFH-1.1 and MA/JFH-1.2). The junction of JFH-1 and MA in the 5′ UTR is an AgeI site, and the junction of MA and JFH-1 in the NS2 region is a BsaBI site. A, AgeI; B, BsaBI; X, XbaI. (B to E) Chimeric HCV RNA replication in Huh7.5.1 cells. HCV core protein level in cells (B) and culture medium (C) and HCV RNA levels in medium (D) and infectivity of culture medium (E) from HCV RNA-transfected Huh7.5.1 cells are shown. Ten micrograms of HCV RNA was transfected into Huh7.5.1 cells, and cells and culture medium were harvested on days 1, 2, and 3. n.d., not determined. Assays were performed three times independently, and data are presented as means ± standard deviation. Dashed line indicates detection limit. wt, wild type.

GGA AGT TCT GCT CGG CCC T-3′ (sense) and 5′-AGA ACT TCC CCA CCT AGC CTC GCG GAA ACC G-3′ (antisense); T1106A, 5′-CAG ATG TAC GCC AGC GCA GAG GGG GAC CTC-3′ (sense) and 5′-CTG CGC TGG CGT ACA TCT GGG TGA CTG GTC-3′ (antisense); and V1951A, 5′-GTG ACG CAG GCG TTA AGC TCA CTC ACA ATT ACC-3′ (sense) and 5′-TGA GCT TAA CGC CTG CGT CAC GCG CAG CGA G-3′ (antisense). To construct the MA chimeric virus harboring minimal regions of JFH-1 (MA/N3H+N5BX-JFH1), ClaI (nt 3930), EcoT22I (nt 5294), and BsrGI (nt 7782) recognition sites were introduced into pMA by site-directed mutagenesis. The 5′ UTR (EcoRI-AgeI), the region of the NS3 helicase (N3H; ClaI-EcoT22I), and the region of NS5B to 3′ X (N5BX; BsrGI-XbaI) were then replaced with the corresponding regions from JFH-1.

RNA synthesis, transfection, and determination of infectivity. RNA synthesis and transfection were performed as described previously (12, 22). Determination of infectivity was also performed as described previously, with infectivity expressed as the number of focus-forming units per milliliter (FFU/ml) (12, 22). When necessary, culture medium was concentrated 20-fold in Amicon Ultra-15 spin columns (100-kDa molecular-weight-cutoff; Millipore, Bedford, MA) in order to determine infectivity.

Quantification of HCV core protein and HCV RNA. In order to estimate the concentration of HCV core protein in culture medium, we performed a chemiluminescence enzyme immunoassay (Lumipulse II HCV core assay; Fujirebio, Tokyo, Japan) in accordance with the manufacturer's instructions. HCV RNA from harvested cells or culture medium was isolated using an RNeasy Mini RNA kit (Qiagen, Tokyo, Japan) or QiaAmp Viral RNA Minikit (Qiagen), respectively. Copy number of HCV RNA was determined by real-time quantitative reverse transcription-PCR (qRT-PCR), as described previously (28).

HCV sequencing. Total RNA in culture supernatant was extracted with Isogen-LS (Nippon Gene Co., Ltd., Tokyo, Japan). cDNA was synthesized using Superscript III Reverse Transcriptase (Invitrogen, Carlsbad, CA). cDNA was subsequently amplified with LA *Taq* DNA polymerase (TaKaRa, Shiga, Japan). Four separate PCR primer sets were used to amplify the fragments of nt 130 to 2909, 2558 to 5142, 4784 to 7279, and 7081 to 9634 covering the entire open reading frame and part of the 5′ UTR and 3′ UTR of the MA strain. Sequences of amplified fragments were determined directly.

Immunostaining. Infected cells were cultured on Multitest Slides (MP Biomedicals, Aurora, OH) and were fixed in acetone-methanol (1:1, vol/vol) for 15 min at −20°C. After a blocking step, infected cells were visualized with anti-core protein antibody (clone 2H9) (29) and Alexa Fluor 488 goat anti-mouse IgG (Invitrogen), and nuclei were visualized with 4′,6′-diamidino-2-phenylindole (DAPI).

Assessment of interferon sensitivity. Two micrograms of *in vitro* transcribed RNA was transfected into 3×10^6 Huh7.5.1 cells. Four hours after transfection, cells were placed in fresh medium or medium containing 0.1, 1, 10, 100, and 1,000 IU/ml of interferon α-2b (Intron A; Schering-Plough Corporation, Osaka, Japan). Culture medium was then harvested on day 3, and HCV core levels in the cells and in the medium were measured.

Statistical analysis. Significant differences were evaluated by Student's *t* test. A P value of <0.05 was considered significant.

RESULTS

Transient replication and production of 2b/2a chimeric virus. We first tested whether the MA strain (genotype 2b) (19) was able to replicate and produce infectious virus in cultured cells. When the *in vitro* transcribed RNA of MA was transfected into Huh7.5.1 cells, a highly HCV-permissive cell line, replication and virus production were not observed (Fig. 1A to C). We then tested whether 2b/2a chimeric RNA harboring the structural region (5′ UTR to E2) of the MA strain and the nonstructural region (p7 to 3′ UTR) of JFH-1 (Fig. 1A, MA/JFH-1.1) was able to replicate in the cells. After MA/JFH-1.1 RNA transfection, time-dependent accumulation of core protein in the cells (Fig. 1B) and culture medium (Fig. 1C) was observed, indicating that MA/JFH-1.1 RNA was able to replicate in the cells autonomously. HCV RNA levels in the medium were determined by qRT-PCR, and time-dependent increases in HCV RNA level were also observed (Fig. 1D). Infectious virus production was observed on day 3, but infectivity was 17.6-fold lower than that of JFH-1 (Fig. 1E).

In order to improve the level of infectious virus production, we tested another chimeric construct, MA/JFH-1.2, which contained an additional MA-to-JFH-1 replacement of the 5′ UTR (Fig. 1A),

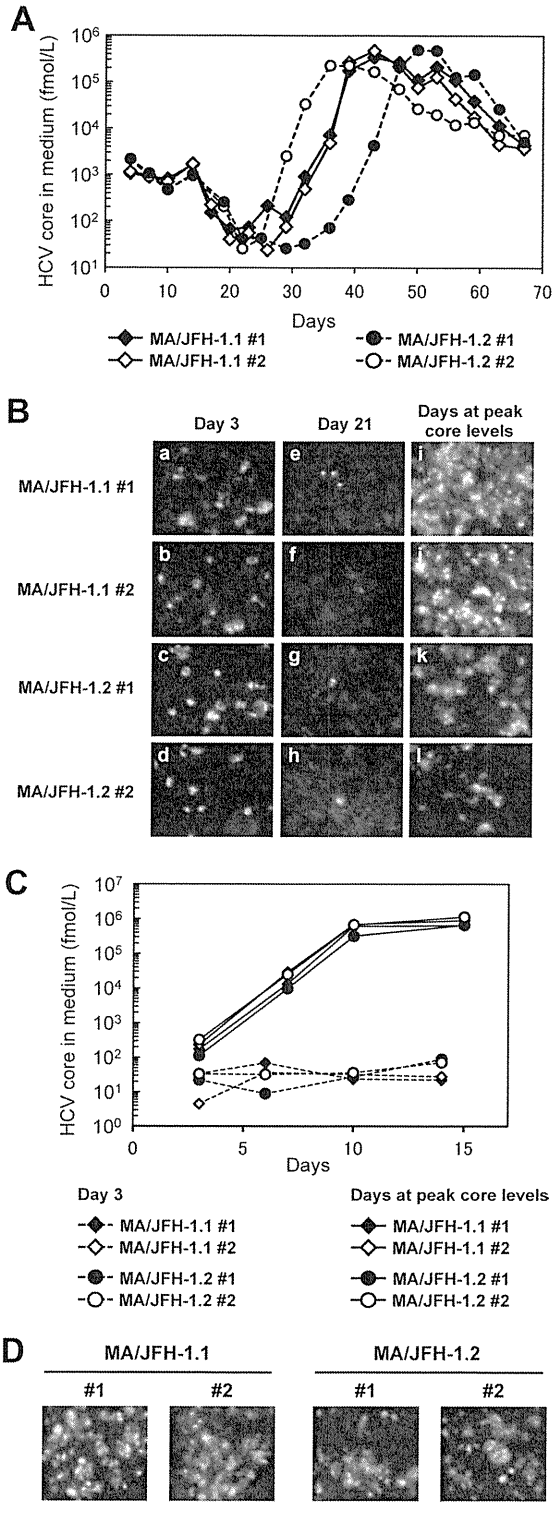

FIG 2 Long-term culture of MA/JFH-1.1 and MA/JFH-1.2 RNA-transfected cells. Ten micrograms of HCV RNA was transfected into Huh7.5.1 cells, and cells were passaged every 2 to 5 days, depending on cell status. Culture medium was collected after every passage, and HCV core protein levels were measured. Transfection was performed twice for each chimeric RNA (1 and 2 for each construct). (A) HCV core protein levels in culture medium from MA/JFH-1.1 and MA/JFH-1.2 RNA-transfected cells. (B) Immunostained cells at 3 days after transfection (a to d), at 21 days after transfection (e to h), and at the time of peak core levels (days 42 to 49). Infected cells were visualized with anti-core protein antibody (green), and nuclei were visualized with DAPI (blue). (C) Infection of naïve cells by culture medium at an MOI of 0.001. (D) Immunostained cells at 15 days after infection with medium at peak core protein levels (Fig. 2A) at an MOI of 0.001. Infected cells were visualized with anti-core antibody (green), and nuclei were visualized with DAPI (blue).

TABLE 1 HCV core protein levels and infectivity in culture medium immediately after RNA transfection (day 3) and after long-term culture (days 35 to 49)

Sample period and virus	Sample no.	Day no.[a]	HCV core (fmol/liter)	Infectivity (FFU/ml)
After transfection				
MA/JFH-1.1	1	3	1.06×10^3	5.00×10^1
	2	3	1.14×10^3	5.70×10^1
MA/JFH-1.2	1	3	2.14×10^3	7.30×10^1
	2	3	2.15×10^3	9.30×10^1
After long-term culture				
MA/JFH-1.1	1	42	3.38×10^5	1.62×10^5
	2	42	4.70×10^5	3.23×10^5
MA/JFH-1.2	1	35	2.27×10^5	1.61×10^5
	2	49	4.93×10^5	3.27×10^5

[a] For the long-term culture, the days are those of peak core protein levels.

as a 5′ UTR replacement from J6CF (genotype 2a) to JFH-1 enhanced virus production of chimeric J6CF virus harboring the region of NS2 to 3′ X of JFH-1 (J6/JFH-1) (A. Murayama et al., unpublished data). The core protein accumulation levels with MA/JFH-1.2 RNA-transfected cells were higher than those with MA/JFH-1.1 ($P < 0.05$) (Fig. 1B). Similarly, core protein and HCV RNA levels in the medium of MA/JFH-1.2 RNA-transfected cells were higher than those of MA/JFH-1.1 ($P < 0.05$) (Fig. 1C and D). Infectivity on day 3 was also higher than with MA/JFH-1.1 ($P < 0.05$) (Fig. 1E), indicating that the 5′ UTR of JFH-1 enhanced virus production. However, infectivity of medium from MA/JFH-1.2 RNA-transfected cells on day 3 remained 6.4-fold lower than that of JFH-1 although HCV RNA levels in the medium were similar to those of JFH-1 (Fig. 1D and E).

These results indicate that 2b/2a chimeric RNA is able to replicate autonomously in Huh7.5.1 cells and produce infectious virus although infectivity remains lower than that of JFH-1.

Assembly-enhancing mutation in core region introduced during long-term culture. Because MA/JFH-1.1 and MA/JFH-1.2 replicated efficiently but produced small amounts of infectious virus, we performed long-term culture of these RNA-transfected cells in order to examine whether these chimeric RNAs would continue replicating and producing infectious virus over the long term. We prepared two RNA-transfected cell lines for each construct (MA/JFH-1.1 and MA/JFH-1.2) as both of these replicated and produced infectious virus at different levels.

Immediately after transfection, core protein levels and infectivity in culture medium were low (1.06×10^3 to 2.15×10^3 fmol/liter and 5.00×10^1 to 9.30×10^1 FFU/ml, respectively) (Fig. 2A and Table 1) although a considerable number of core protein-positive cells were observed by immunostaining (Fig. 2B, frames a to d). Subsequently, core protein levels in the culture medium decreased gradually (Fig. 2A), and core protein-positive cells were rare (Fig. 2B, frames e to h). However, at 30 to 40 days

after transfection, core protein levels in the supernatants of all chimeric RNA-transfected cells increased and reached 2.27×10^5 to 4.93×10^5 fmol/liter (Fig. 2A and Table 1). Infectivity in the culture medium also increased (1.61×10^5 to 3.27×10^5 FFU/ml) (Table 1), and at this point, most of the cells were core protein positive (Fig. 2B, frame i to l).

As the infectivity of culture supernatant of MA/JFH-1 RNA-transfected cells appeared to increase after long-term culture, we compared viral spread by infection with these supernatants on day 3 (immediately after transfection) and for each peak in core protein levels (after long-term culture). When naïve Huh7.5.1 cells were infected with supernatant on days corresponding to a peak in core protein levels at a multiplicity of infection (MOI) of 0.001, core protein levels in the medium increased rapidly and reached 0.64×10^6 to 1.13×10^6 fmol/liter by day 15 after infection (Fig. 2C). Immunostained images showed that most cells were HCV core protein positive on day 15 (Fig. 2D). When naïve Huh7.5.1 cells were infected with supernatant from day 3 at an MOI of 0.001, core protein levels in the medium did not increase under these conditions (Fig. 2C). These results indicate that both MA/JFH-1 chimeric viruses (MA/JFH-1.1 and MA/JFH-1.2) acquired the ability to spread rapidly after long-term culture.

As the characteristics of the MA/JFH-1 virus changed in long-term culture, we analyzed the possible mutations in the viral genome from the supernatant at each peak in core protein levels (Table 1, days at peak core levels). Nine- to 12-nucleotide mutations were found in the viral genome from each supernatant, and the detected mutations were distributed along the entire genome. Among these mutations, a common nonsynonymous mutation was found in the core region (Arg to Gly at amino acid [aa]167, R167G).

In order to test the effects of R167G on virus production, an R167G substitution was introduced into MA/JFH-1.2 as MA/JFH-1.2 replicated and produced infectious virus more efficiently than MA/JFH-1.1. HCV core protein levels in cells and medium of MA/JFH-1.2 with R167G (MA/JFH-1.2/R167G) were higher than with MA/JFH-1.2 ($P < 0.05$) (Fig. 3A and B). HCV RNA levels in the medium of MA/JFH-1.2/R167G RNA-transfected cells were also higher than with MA/JFH-1.2 ($P < 0.05$) (Fig. 3C). Infectious virus production was also increased by the R167G mutation ($P < 0.05$) (Fig. 3D) and was 8.7-fold higher than that of JFH-1 RNA-transfected cells on day 3 ($P < 0.05$) (Fig. 3D).

We then tested whether R167G was responsible for the rapid spread observed in culture supernatant after long-term culture by monitoring virus spread after infection of naïve Huh7.5.1 with culture medium taken 3 days after RNA transfection of MA/JFH-1.2 and MA/JFH-1.2/R167G at an MOI of 0.005. Core protein levels in medium from MA/JFH-1.2/R167G-infected cells increased with the same kinetics as levels of JFH-1 (Fig. 3E), and the population of core protein-positive cells was almost the same as with JFH-1-infected cells (Fig. 3F), indicating that MA/JFH-1.2/R167G virus spread as rapidly as JFH-1 virus. In contrast, we observed no infectious foci in the MA/JFH-1.2 virus-inoculated cells (Fig. 3F). These data suggest that the R167G mutation in the core region was a cell culture-adaptive mutation and that it enhanced infectious MA/JFH-1.2 virus production.

In order to determine whether R167G enhances RNA replication or other steps in the viral life cycle, we performed a single-cycle virus production assay (11) using Huh7-25 cells, a HuH-7-derived cell line lacking CD81 expression on the cell surface (1).

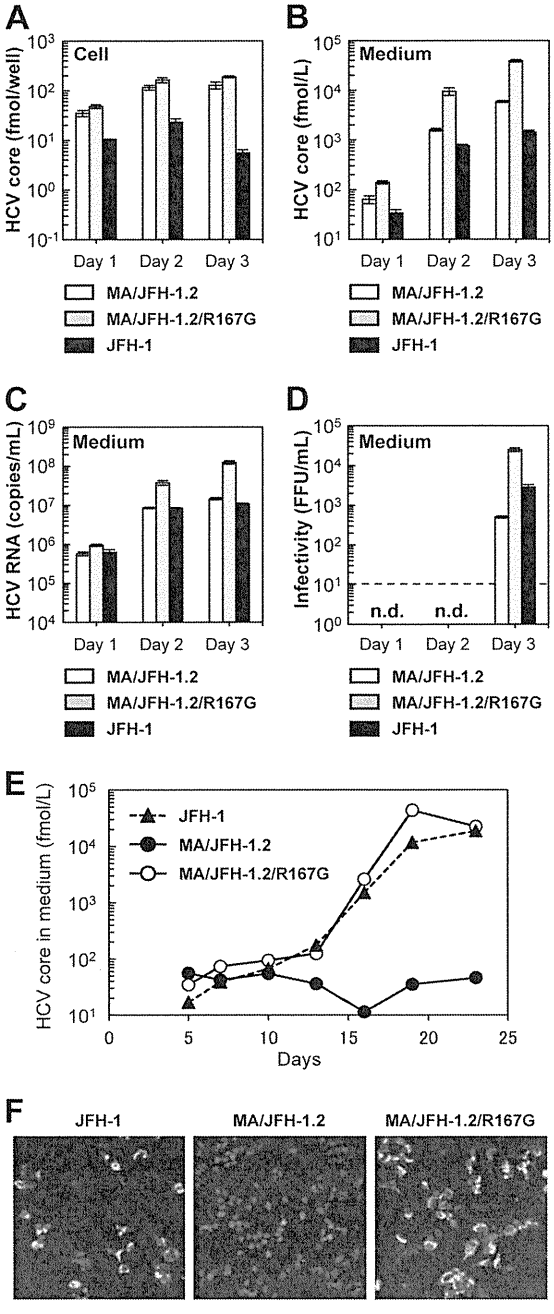

FIG 3 Effects of R167G on replication and virus production of MA/JFH-1.2 in Huh7.5.1 cells. Ten micrograms of HCV RNA was transfected into Huh7.5.1 cells, and cells and medium were harvested on days 1, 2, and 3. HCV core protein levels in the cells (A) and culture medium (B) and HCV RNA levels in the medium (C) and the infectivity of culture medium (D) from HCV RNA-transfected Huh7.5.1 cells are shown. n.d., not determined. Dashed line indicates the detection limit. Assays were performed three times independently, and data are presented as means ± standard deviation. (E) HCV core protein levels in culture medium from cells infected with medium at 3 days posttransfection at an MOI of 0.005. (F) Immunostained cells at 19 days postinfection. Infected cells were visualized with anti-core antibody (green), and nuclei were visualized with DAPI (blue).

This cell line can support replication and infectious virus production upon transfection of HCV genomic RNA but cannot be reinfected by progeny virus, thereby allowing observation of a single cycle of infectious virus production without the confounding ef-

fects of reinfection. R167G did not affect HCV core protein levels in the chimeric RNA-transfected Huh7-25 cells (Fig. 4A), demonstrating that R167G did not enhance RNA replication. Nevertheless, R167G increased HCV core protein levels in the medium ($P < 0.05$ on days 2 and 3) and infectivity (Fig. 4B and C). These results suggest that R167G did not affect RNA replication but affected other steps such as virus assembly and/or virus secretion.

Virus particle assembly efficiency was then assessed by determining intracellular-specific infectivity from infectivity and RNA titer in the cells, as reported previously (11). As shown in Fig. 4G, R167G enhanced intracellular-specific infectivity of MA/JFH-1.2 virus 10.2-fold. Virus secretion efficiency was also calculated from the amount of intracellular and extracellular infectious virus, but R167G had no effect (Fig. 4G).

To confirm the effects of Arg167 in other HCV strains, we tested its effects on JFH-1. As aa 167 of JFH-1 is Gly, we replaced it with Arg (G167R). HCV core protein levels in the cells were not affected by G167R (Fig. 4D), and no effects on RNA replication were confirmed. HCV core protein levels in the medium and infectivity decreased after G167R mutation (Fig. 4E and F). As the G167R mutation decreased intracellular infectious virus production of JFH-1 to undetectable levels, we were unable to determine the intracellular-specific infectivity and virus secretion efficiency of JFH-1 G167R (Fig. 4G). These results indicate that Gly is favored over Arg at core position 167 for infectious virus assembly in multiple HCV strains.

MA harboring the R167G mutation, 5′ UTR, and N3H (NS3 helicase) and N5BX (NS5B to 3′ X) regions of JFH-1 replicated and produced infectious chimeric virus. In order to establish a genotype 2b cell culture system with the MA strain with minimal regions of JFH-1, we attempted to reduce JFH-1 content in MA/JFH-1.2. We previously reported that replacement of the N3H and N5BX regions of JFH-1 allowed efficient replication of the J6CF strain, which normally cannot replicate in cells (21). Thus, we tested whether the N3H and N5BX regions of JFH-1 could also support MA RNA replication.

We prepared two chimeric MA constructs harboring the 5′ UTR and N3H and N5BX regions of JFH-1, MA/N3H+N5BX-JFH1 (Fig. 5A) and MA/N3H+N5BX-JFH1/R167G. After *in vitro* transcribed RNA was transfected into Huh7.5.1 cells, intracellular core protein levels of MA/N3H+N5BX-JFH1 and MA/N3H+N5BX-JFH1/R167G RNA-transfected cells increased in a time-dependent manner and reached almost the same levels as with MA/JFH-1.2 RNA-transfected cells on day 5 (Fig. 5B). Extracellular core protein and HCV RNA levels of MA/N3H+N5BX-JFH1 and MA/N3H+N5BX-JFH1/R167G RNA-transfected cells also increased in a time-dependent manner (Fig. 5C and D). However, they were more than 10 times lower than with MA/JFH-1.2 RNA-transfected cells although intracellular core levels were comparable on day 5 (Fig. 5B to D).

We then tested whether the medium from MA/N3H+N5BX-JFH1 and MA/N3H+N5BX-JFH1/R167G RNA-transfected cells was infectious. Infectivity of the medium from MA/N3H+N5BX-JFH1 RNA-transfected cells was below the detection limit, and that of MA/N3H+N5BX-JFH1/R167G RNA-transfected cells on day 5 was very low ($3.3 \times 10^1 \pm 2.1 \times 10^1$ FFU/ml) (Fig. 5E). To confirm infectivity, the culture media were concentrated, and their infectivity was determined. Infected foci were observed after infection with concentrated medium in MA/N3H+N5BX-JFH1/R167G RNA-transfected cells (Fig. 5F), and infectivity was found

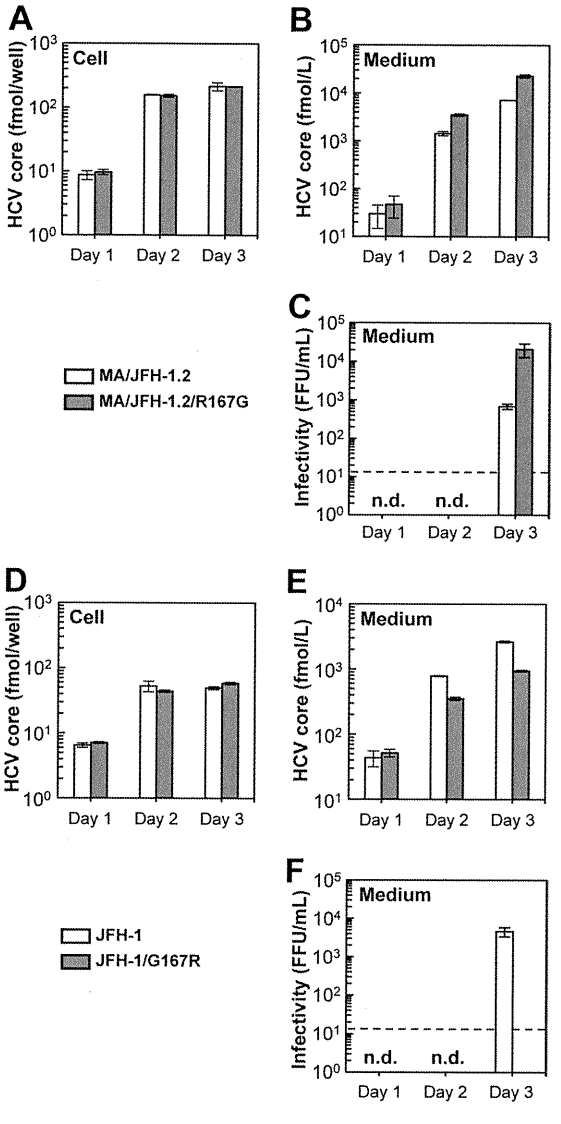

G

Construct	Intracellular Specific Infectivity (FFU/ x10⁶ HCV RNA copies)	Infectious Virus Secretion (Extra/Intra)
MA/JFH-1.2	1.68 ± 0.404	20.2 ± 4.26
MA/JFH-1.2/R167G	17.1 ± 4.38	14.1 ± 1.65
JFH-1	1.78 ± 0.364	63.3 ± 6.44
JFH-1/G167R	NA	NA

FIG 4 Effects of R167G on replication and virus production of MA/JFH-1.2 and JFH-1 in Huh7-25 cells. Ten micrograms of HCV RNA was transfected into Huh7-25 cells, and cells and medium were harvested on days 1, 2, and 3. HCV core protein levels in cells (A and D) and in medium (B and E) were measured, and infectivity of medium (C and F) was determined. n.d., not determined. Dashed line indicates the detection limit. (G) Intracellular specific infectivity and virus secretion efficiency of chimeric HCV RNA-transfected cells. Intracellular and extracellular infectivity of day 3 samples was determined, and specific infectivity and virus secretion rate were calculated. Assays were performed three times independently, and data are presented as means ± standard deviation. NA, not available.

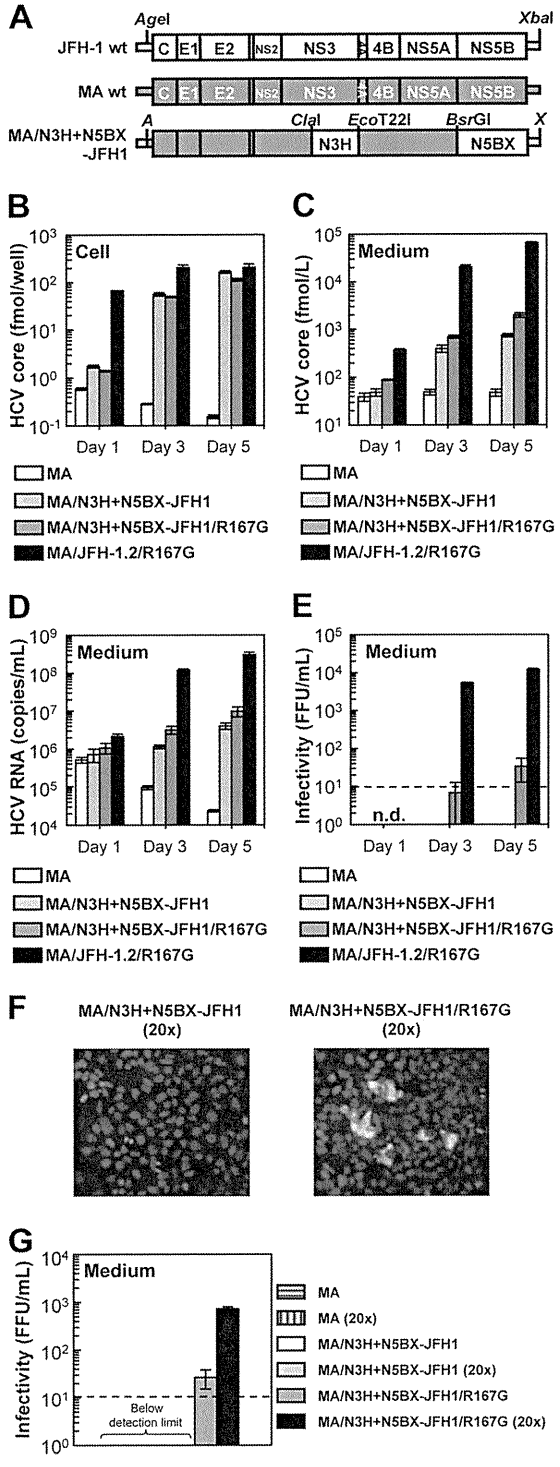

FIG 5 Replication and virus production of MA/N3H+N5BX-JFH1/R167G in Huh7.5.1 cells. (A) Schematic structures of JFH-1, MA, and MA/N3H+N5BX-JFH1. The junction of JFH-1 and MA in the 5′ UTR is an AgeI site; the junctions of MA and JFH-1 in the NS3 regions are ClaI and EcoT22I sites, and the junction in the NS5B region is a BsrGI site. A, AgeI; X, XbaI. (B to G) Chimeric HCV RNA replication in Huh7.5.1 cells. Ten micrograms of HCV RNA was transfected into Huh7.5.1 cells, and cells and medium were harvested on days 1, 3, and 5. HCV core protein levels in cells (B) and in medium (C) and HCV RNA levels in medium (D) were measured, and infectivity of medium (E) was determined. Assays were performed three times independently, and data are presented as means ± standard deviation. n.d., not determined. Dashed line indicates the detection limit. (F) Immunostained cells. Huh7.5.1 cells were infected with concentrated medium from RNA-transfected cells on day 5. Infected cells were visualized with anti-core antibody (green), and nuclei were visualized with DAPI (blue). (G) Infectivity of concentrated culture medium from HCV RNA-transfected cells. Culture medium was concentrated by 20 times. Infectivities of original and concentrated culture media were determined. Dashed line indicates detection thelimit.

to be $7.27 \times 10^2 \pm 7.57 \times 10^1$ FFU/ml (Fig. 5G). No infected foci were observed after infection of MA/N3H+N5BX-JFH1 RNA-transfected cells, even when medium was concentrated (Fig. 5F), although intracellular and extracellular core protein levels were comparable to those with MA/N3H+N5BX-JFH1/R167G RNA-transfected cells (Fig. 5B and C). These results indicate that replacement of the 5′ UTR and N3H and N5BX regions in JFH-1 were necessary to rescue autonomous replication in the replication-incompetent MA strain and for secretion of infectious chimeric virus. However, the secretion and infection efficiencies of the virus were low.

Cell culture-adaptive mutations enhanced infectious virus production of MA/N3H+N5BX-JFH1/R167G. Because MA/N3H+N5BX-JFH1/R167G replicated efficiently but produced very small amounts of infectious virus, we performed a long-term culture of the RNA-transfected cells in order to induce cell culture-adaptive mutations that could enhance infectious virus production. We prepared RNA-transfected cells using two constructs, MA/N3H+N5BX-JFH1 and MA/N3H+N5BX-JFH1/R167G; both of these replicated efficiently, and MA/N3H+N5BX-JFH1/R167G produced infectious virus at low levels while MA/N3H+N5BX-JFH1 did not. Immediately after transfection, the HCV core protein levels in the medium of each RNA-transfected cell culture peaked at 3.0×10^3 fmol/liter and declined thereafter. However, the core protein level in the medium with MA/N3H+N5BX-JFH1/R167G RNA-transfected cells continued to increase and reached a peak of 2.7×10^5 fmol/liter 54 days after transfection, at which point most cells were core protein positive (Fig. 6B). The core protein level in the medium with MA/N3H+N5BX-JFH1 RNA-transfected cells did not increase and core-positive cells were scarce on day 54 (Fig. 6B). We analyzed the viral genome in the culture supernatants from day 54 for possible mutations and identified four nonsynonymous mutations in the MA/N3H+N5BX-JFH1/R167G genome: L814S (NS2), R1012G, (NS2), T1106A (NS3), and V1951A (NS4B). In order to test whether these amino acid substitutions enhance infectious virus production, L814S, R1012G, T1106A, and V1951A were introduced into MA/N3H+N5BX-JFH1/R167G, and the product was designated MA/N3H+N5BX-JFH1/5am (where am indicates adaptive mutation). On day 1, although HCV core protein levels in the MA/N3H+N5BX-JFH1/5am RNA-transfected cells were higher than those of MA/N3H+N5BX-JFH1/R167G RNA-transfected cells, they were still lower than those of MA/JFH-1.2/R167G RNA-transfected cells; however, on days 3 and 5, they reached a level comparable to that of MA/JFH-1.2/R167G RNA-transfected cells (Fig. 6C). HCV core protein and HCV RNA levels in the medium of MA/N3H+N5BX-JFH1/5am RNA-transfected cells were higher than those of MA/JFH-1.2/R167G RNA-transfected cells ($P < 0.05$, Fig. 6D and 6E, respectively). MA/N3H+N5BX-JFH1/5am, containing the four additional adaptive mutations, produced infectious virus at the same level as MA/JFH-1.2/R167G on day 5 (Fig. 6F). These results indicate that the

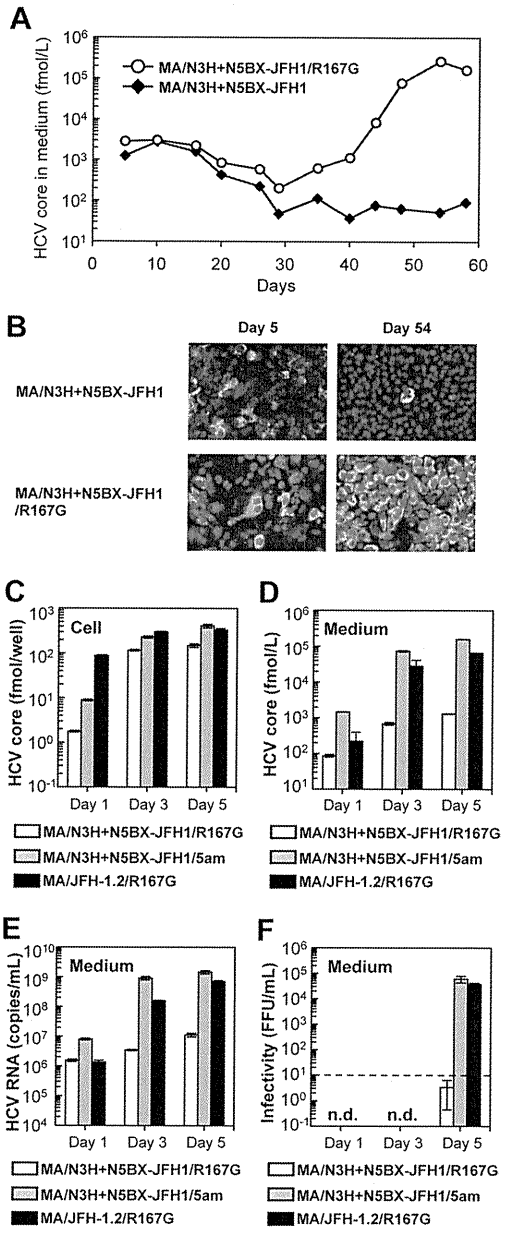

FIG 6 Cell culture-adaptive mutations enhanced infectious virus production of MA/N3H+N5BX-JFH1/R167G. (A) Long-term culture of MA/N3H+N5BX-JFH1 and MA/N3H+N5BX-JFH1/R167G RNA-transfected cells. Ten micrograms of HCV RNA was transfected into Huh7.5.1 cells, and cells were passaged every 2 to 5 days, depending on cell status. Culture medium was collected after every passage, and HCV core protein levels were measured. HCV core protein levels in culture medium from MA/N3H+N5BX-JFH1 and MA/N3H+N5BX-JFH1/R167G RNA-transfected cells are presented. (B) Immunostained cells on days 5 and 54 after transfection. Infected cells were visualized with anti-core antibody (green), and nuclei were visualized with DAPI (blue). (C to F) Effect of four additional cell culture-adaptive mutations on virus production. Ten micrograms of HCV RNA was transfected into Huh7.5.1 cells, and cells and medium were harvested on days 1, 3, and 5. HCV core levels in cells (C) and in medium (D) and HCV RNA levels in medium (E) were measured, and infectivity of medium (F) was determined. Assays were performed three times independently, and data are presented as means ± standard deviation. n.d., not determined. Dashed line indicates the detection limit.

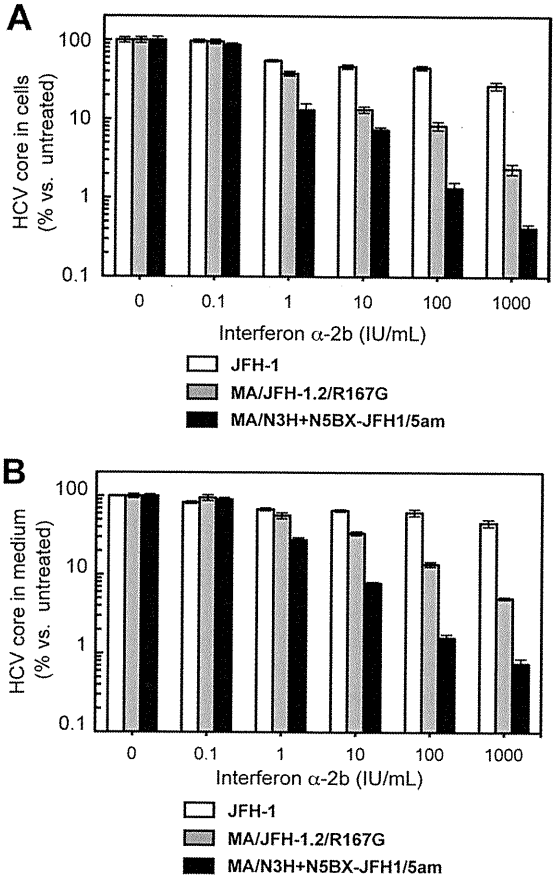

FIG 7 Comparisons of interferon sensitivity between JFH-1, MA/JFH-1.2/R167G and MA/N3H+N5BX-JFH1/5am. Two micrograms of HCV RNA was transfected into Huh7.5.1 cells, and interferon was added at the indicated concentrations at 4 h after transfection. HCV core protein levels in cells (A) and in medium (B) on day 3 were measured, and data are expressed as percent versus untreated cells (0 IU/ml). Assays were performed three times independently, and data are presented as means ± standard deviation.

four additional adaptive mutations enhance infectious virus production and that MA/N3H+N5BX-JFH1/5am RNA-transfected cells replicate and produce infectious virus as efficiently as MA/JFH-1.2/R167G RNA-transfected cells.

Comparison of interferon sensitivity between JFH-1, MA/JFH-1.2/R167G, and MA/N3H+N5BX-JFH1/R167G. Using the newly established genotype 2b infectious chimeric virus, we compared interferon sensitivity between the JFH-1, MA/JFH-1.2/R167G, and MA/N3H+N5BX-JFH1/5am viruses. JFH-1 or MA chimeric viral RNA-transfected Huh7.5.1 cells were treated with 0.1, 1, 10, 100, or 1,000 IU/ml interferon α-2b, and HCV core protein levels in the cells and in culture media were compared. Interferon decreased HCV core protein levels in the JFH-1 RNA-transfected cells and in the medium in a dose-dependent manner, and production was inhibited to 26.8% ± 3.0% and 45.6% ± 4.7%, respectively, of control levels (Fig. 7A and B, respectively). In contrast, HCV core protein levels in cells and medium of MA/JFH-1.2/R167G and MA/N3H+N5BX-JFH1/5am RNA-transfected cells decreased more pronouncedly in a dose-dependent manner (Fig. 7A and B, respectively). HCV core protein levels in cells and medium from MA/N3H+N5BX-JFH1/5am RNA-transfected cells were lower than those from MA/JFH-1.2/

R167G RNA-transfected cells (Fig. 7A and B, respectively) ($P < 0.05$ at 1, 10, 100, and 1,000 IU/ml), indicating that the MA/N3H+N5BX-JFH1/5am virus was more sensitive to interferon than the MA/JFH1.2/R167G virus, which contained more regions from JFH-1.

DISCUSSION

In this study, we developed a novel infectious HCV production system using a genotype 2b chimeric virus. To improve infectious virus production, we introduced two modifications into the chimeric genome.

First, we replaced the 5′ UTR from MA with that of JFH-1. Similarly to J6/JFH-1, replacement of the 5′ UTR increased core protein accumulation in both the cells and medium when these RNAs were transfected into Huh7.5.1 cells (Fig. 1). The same trend was observed when these RNAs were transfected into Huh7-25 cells (data not shown), indicating that the 5′ UTR of JFH-1 enhanced RNA replication. There are two genetic variations in J6CF and seven in MA in the region we replaced (nt 1 to 154 for J6CF and nt 1 to 155 for MA), and some of these mutations may affect RNA replication by changing the RNA secondary structure, RNA-RNA interactions, or binding of host or viral proteins.

Second, we introduced a cell culture-adaptive mutation (R167G) in the core region. This mutation was induced by long-term culture of MA/JFH-1 RNA-transfected cells (Fig. 2). MA/JFH-1 chimeric RNA (MA/JFH-1.1 and MA/JFH-1.2) replicated when synthesized RNA was transfected into the cells. However, infectious virus production was low, and virus infection did not spread over the short term. In early stages of long-term culture, the number of core protein-positive cells gradually decreased, and core protein-positive cells were scarcely detectable. Subsequently, the population of core protein-positive cells increased, reaching almost 100%. At this time point, we identified a common mutation in the core region (R167G) of the viral genome as a cell culture-adaptive mutation and found that it enhanced infectious virus production (Fig. 3). Several nonsynonymous mutations other than R167G were identified in the viral genome from each supernatant, and these mutations may enhance infectious virus production. However, there was a discrepancy between RNA levels and the infectivity of the culture media of MA/JFH-1.2 and MA/JFH-1.2/R167G RNA-transfected cells (Fig. 3C and D). The MA/JFH-1.2/R167G mutant had a 2-log increase in viral infectivity compared to that of MA/JFH-1.2 but only a 1-log increase in secreted RNA. The replication efficiency of MA/JFH-1.2 RNA-transfected cells was comparable to that of MA/JFH-1.2/R167G RNA-transfected cells, but the efficiency of infectious virus assembly within the cells was low, indicating that mainly noninfectious virus may be produced.

Infection of MA/JFH-1.2/R167G virus spreads rapidly, similarly to that of the JFH-1 virus, when it is inoculated into naïve Huh7.5.1 cells. On a single-cycle virus production assay, we found that the R167G mutation did not affect RNA replication or virus secretion but enhanced infectious virus assembly within the cells (Fig. 4). Efficient infectious virus assembly within the cells was mainly responsible for the rapid spread and high virus production of MA/JFH-1.2/R167G.

The amino acid at 167 (aa 167) is located in domain 2 of the core region, which is important for localization of the core protein (3, 8). Lipid droplet localization of the core protein and/or NS5A is important for infectious virus production (4, 18, 26). The interaction between the core protein and NS5A is also important for infectious virus production (16). Thus, aa 167 affects infectious virus production possibly by altering subcellular localization of the core protein or interaction between the core protein and NS5A. We examined the amino acid sequence of the core protein in 2,078 strains in the Hepatitis Virus Database (http://s2as02.genes.nig.ac.jp/) and found that aa 167 is Gly in all other strains. These data strongly suggest that Gly at aa 167 is important for the HCV life cycle. As the MA strain was cloned from the serum of a patient with chronic hepatitis C, the low virus production by this Gly at aa 167 may be important for persistent infection.

We then attempted to reduce the contents of JFH-1 from MA/JFH-1.2/R167G. We previously reported that the N3H and N5BX regions of JFH-1 were sufficient for replication of the J6CF strain (21). We also reported that this effect was observed only in genotype 2a strains (J6CF, JCH-1, and JCH-4). In this study, we tested whether the N3H and N5BX regions of JFH-1 could also support replication of a genotype 2b strain, MA. We constructed an MA chimeric virus harboring the N3H and N5BX regions of JFH-1 and combined this with the 5′ UTR of JFH-1 and the R167G mutation (MA/N3H+N5BX-JFH1/R167G). This chimeric RNA was able to replicate in the cells and produce infectious chimeric virus in culture medium although infectious virus production levels were low (Fig. 5).

We showed in this paper that the N3H and N5BX regions of JFH-1 were able to support RNA replication by both genotype 2a clones and genotype 2b clones, but the nucleotide sequence similarity between JFH-1 and MA was lower than that between JFH-1 and J6CF (77% versus 89%, respectively). Compared to MA/JFH-1.2/R167G, MA/N3H+N5BX-JFH1/R167G RNA showed the same levels of RNA replication and low levels of infectious virus production. To clarify whether there were any differences in the characteristics of the secreted virus, we performed density gradient ultracentrifugation with the MA/JFH-1.2/R167G and MA/N3H+N5BX-JFH1/R167G viruses. The distributions of the HCV core protein and infectivity showed similar profiles (data not shown).

The differences between MA/JFH-1.2/R167G and MA/N3H+N5BX-JFH1/R167G are the NS2, NS3 protease domain (N3P), and NS4A to NS5A regions. Nucleotide variation(s) other than aa 167 in these regions of the MA strain may be associated with reduced virus assembly. We identified four additional cell culture-adaptive mutations, L814S (NS2), R1012G (NS2), T1106A (NS3), and V1951A (NS4B), which resulted from long-term culture of MA/N3H+N5BX-JFH1/R167G RNA-transfected cells. Consequently, cells transfected with MA/N3H+N5BX-JFH1/5am constructed by insertion of these four adaptive mutations into MA/N3H+N5BX-JFH1/R167G replicated and produced infectious virus as efficiently as MA/JFH-1.2/R167G RNA-transfected cells (Fig. 6).

This system is able to contribute to studies into the development of antiviral strategies. It has been reported that HCV genotype 2a was more sensitive to interferon therapy than HCV genotype 2b in a clinical study (20). To assess the interferon resistance of genotype 2b, a cell culture system with multiple genotype 2b strains is necessary. The previously reported replicable genotype 2b chimeric virus harbored only structural

regions of 2b strains (6, 27). The 2b/JFH-1 chimeric virus containing the region of the core protein to NS2 from the J8 strain (genotype 2b) and the region of NS3 to 3′ X of JFH-1 was able to replicate and showed that there were no differences in interferon sensitivity among the JFH-1 chimeric viruses of other genotypes (6, 27). Another 2b/JFH-1 chimeric virus containing the regions of the core protein to NS2 (nt 342 to 2867) of a genotype 2b strain and of NS2 to 3′ UTR (nt 2868) of JFH-1 has been reported (6, 27). The authors reported that their 2b/JFH-1 chimeric virus was more sensitive to interferon than JFH-1 (6, 27). We developed the genotype 2b HCV cell culture system with another HCV genotype 2b strain (MA). We identified a virus assembly-enhancing mutation in the core region, the minimal JFH-1 regions necessary for replication, and four additional adaptive mutations that enhance infectious virus production and demonstrated that MA harboring the five adaptive mutations and the 5′ UTR and N3H and N5BX regions of JFH-1 (MA/N3H+N5BX-JFH1/5am) could replicate and produce infectious virus efficiently.

Using these novel genotype 2b chimeric viruses, we assessed interferon sensitivity. We found that MA/JFH-1.2/R167G chimeric virus and MA/N3H+N5BX-JFH1/5am virus were more sensitive to interferon than the JFH-1 virus (Fig. 7). Furthermore, we found that MA/N3H+N5BX-JFH1/5am was more sensitive to interferon than MA/JFH-1.2/R167G, indicating that the genetic variation(s) in the NS2, N3P, and NS4A to NS5A regions affect interferon sensitivity. Although genotype 2a viruses are more sensitive to interferon than genotype 2b viruses in clinical studies, JFH-1 displayed interferon resistance in our study.

These results suggest that the JFH-1 regions in the 2b/JFH-1 virus affect the interferon sensitivity of the chimeric virus. Moreover, it was reported that amino acid variations in E2, p7, NS2, and NS5A were associated with the response to peginterferon and ribavirin therapy in genotype 2b HCV infection (10). Therefore, our MA/JFH-1 chimeric virus harboring minimal regions from JFH-1 (MA/N3H+N5BX-JFH1/5am) is more suitable for assessing the characteristics of the MA strain than the MA/JFH-1 chimeric virus, which includes a nonstructural region from JFH-1 (MA/JFH-1.2/R167G). We showed here that replacement of the 5′ UTR and N3H and N5BX regions in MA with those from JFH-1 is able to convert MA into a replicable virus. Using the same strategy, numerous HCV cell culture systems with various genotype 2b strains, as well as genotype 2a strains, may be available.

In conclusion, we established a novel HCV genotype 2b cell culture system using a chimeric genome in MA harboring minimal regions from JFH-1. This cell culture system using the chimeric genotype 2b virus will be useful for characterization of genotype 2b viruses and the development of antiviral strategies.

ACKNOWLEDGMENTS

We are grateful to Tetsuro Suzuki of Hamamatsu University School of Medicine for helpful comments and suggestions. Huh7.5.1 cells were kindly provided by Francis V. Chisari.

A.M. is partially supported by the Japan Health Sciences Foundation and Viral Hepatitis Research Foundation of Japan. This work was partially supported by Grants-in-Aid for Scientific Research from the Japan Society for the Promotion of Science, from the Ministry of Health, Labor and Welfare of Japan, from the Ministry of Education, Culture, Sports, Science and Technology, from the National Institute of Biomedical Innovation, and by Research on Health Sciences Focusing on Drug Innovation from the Japan Health Sciences Foundation.

REFERENCES

1. **Akazawa D, et al.** 2007. CD81 expression is important for the permissiveness of Huh7 cell clones for heterogeneous hepatitis C virus infection. J. Virol. **81**:5036–5045.
2. **Bartenschlager R, Lohmann V.** 2000. Replication of hepatitis C virus. J. Gen. Virol. **81**:1631–1648.
3. **Boulant S, et al.** 2006. Structural determinants that target the hepatitis C virus core protein to lipid droplets. J. Biol. Chem. **281**:22236–22247.
4. **Boulant S, Targett-Adams P, McLauchlan J.** 2007. Disrupting the association of hepatitis C virus core protein with lipid droplets correlates with a loss in production of infectious virus. J. Gen. Virol. **88**:2204–2213.
5. **Choo QL, et al.** 1989. Isolation of a cDNA clone derived from a blood-borne non-A, non-B viral hepatitis genome. Science **244**:359–362.
6. **Gottwein JM, et al.** 2009. Development and characterization of hepatitis C virus genotype 1–7 cell culture systems: role of CD81 and scavenger receptor class B type I and effect of antiviral drugs. Hepatology **49**:364–377.
7. **Griffin S, et al.** 2008. Genotype-dependent sensitivity of hepatitis C virus to inhibitors of the p7 ion channel. Hepatology **48**:1779–1790.
8. **Hope RG, McLauchlan J.** 2000. Sequence motifs required for lipid droplet association and protein stability are unique to the hepatitis C virus core protein. J. Gen. Virol. **81**:1913–1925.
9. **Jensen TB, et al.** 2008. Highly efficient JFH1-based cell-culture system for hepatitis C virus genotype 5a: failure of homologous neutralizing-antibody treatment to control infection. J. Infect. Dis. **198**:1756–1765.
10. **Kadokura M, et al.** 2011. Analysis of the complete open reading frame of genotype 2b hepatitis C virus in association with the response to peginterferon and ribavirin therapy. PLoS One **6**:e24514.
11. **Kato T, et al.** 2008. Hepatitis C virus JFH-1 strain infection in chimpanzees is associated with low pathogenicity and emergence of an adaptive mutation. Hepatology **48**:732–740.
12. **Kato T, et al.** 2006. Cell culture and infection system for hepatitis C virus. Nat. Protoc. **1**:2334–2339.
13. **Kiyosawa K, et al.** 1990. Interrelationship of blood transfusion, non-A, non-B hepatitis and hepatocellular carcinoma: analysis by detection of antibody to hepatitis C virus. Hepatology **12**:671–675.
14. **Lindenbach BD, et al.** 2005. Complete replication of hepatitis C virus in cell culture. Science **309**:623–626.
15. **Lohmann V, et al.** 1999. Replication of subgenomic hepatitis C virus RNAs in a hepatoma cell line. Science **285**:110–113.
16. **Masaki T, et al.** 2008. Interaction of hepatitis C virus nonstructural protein 5A with core protein is critical for the production of infectious virus particles. J. Virol. **82**:7964–7976.
17. **Miyamoto M, Kato T, Date T, Mizokami M, Wakita T.** 2006. Comparison between subgenomic replicons of hepatitis C virus genotypes 2a (JFH-1) and 1b (Con1 NK5.1). Intervirology **49**:37–43.
18. **Miyanari Y, et al.** 2007. The lipid droplet is an important organelle for hepatitis C virus production. Nat. Cell Biol. **9**:1089–1097.
19. **Murakami K, Abe M, Kageyama T, Kamoshita N, Nomoto A.** 2001. Down-regulation of translation driven by hepatitis C virus internal ribosomal entry site by the 3′ untranslated region of RNA. Arch. Virol. **146**:729–741.
20. **Murakami T, et al.** 1999. Mutations in nonstructural protein 5A gene and response to interferon in hepatitis C virus genotype 2 infection. Hepatology **30**:1045–1053.
21. **Murayama A, et al.** 2007. The NS3 helicase and NS5B-to-3′X regions are important for efficient hepatitis C virus strain JFH-1 replication in Huh7 cells. J. Virol. **81**:8030–8040.
22. **Murayama A, et al.** 2010. RNA polymerase activity and specific RNA structure are required for efficient HCV replication in cultured cells. PLoS Pathog. **6**:e1000885.
23. **Pietschmann T, et al.** 2006. Construction and characterization of infectious intragenotypic and intergenotypic hepatitis C virus chimeras. Proc. Natl. Acad. Sci. U. S. A. **103**:7408–7413.
24. **Pietschmann T, et al.** 2009. Production of infectious genotype 1b virus particles in cell culture and impairment by replication enhancing mutations. PLoS Pathog. **5**:e1000475.
25. **Scheel TK, et al.** 2008. Development of JFH1-based cell culture systems

for hepatitis C virus genotype 4a and evidence for cross-genotype neutralization. Proc. Natl. Acad. Sci. U. S. A. **105**:997–1002.
26. **Shavinskaya A, Boulant S, Penin F, McLauchlan J, Bartenschlager R.** 2007. The lipid droplet binding domain of hepatitis C virus core protein is a major determinant for efficient virus assembly. J. Biol. Chem. **282**: 37158–37169.
27. **Suda G, et al.** 2010. IL-6-mediated intersubgenotypic variation of interferon sensitivity in hepatitis C virus genotype 2a/2b chimeric clones. Virology **407**:80–90.
28. **Takeuchi T, et al.** 1999. Real-time detection system for quantification of hepatitis C virus genome. Gastroenterology **116**:636–642.
29. **Wakita T, et al.** 2005. Production of infectious hepatitis C virus in tissue culture from a cloned viral genome. Nat. Med. **11**:791–796.
30. **Yi M, Ma Y, Yates J, Lemon SM.** 2007. Compensatory mutations in E1, p7, NS2, and NS3 enhance yields of cell culture-infectious intergenotypic chimeric hepatitis C virus. J. Virol. **81**:629–638.
31. **Yi M, Villanueva RA, Thomas DL, Wakita T, Lemon SM.** 2006. Production of infectious genotype 1a hepatitis C virus (Hutchinson strain) in cultured human hepatoma cells. Proc. Natl. Acad. Sci. U. S. A. **103**:2310–2315.
32. **Zhong J, et al.** 2005. Robust hepatitis C virus infection in vitro. Proc. Natl. Acad. Sci. U. S. A. **102**:9294–9299.

Proteomics Analysis of Mitochondrial Proteins Reveals Overexpression of a Mitochondrial Protein Chaperon, Prohibitin, in Cells Expressing Hepatitis C Virus Core Protein

Takeya Tsutsumi,[1] Mami Matsuda,[2] Hideki Aizaki,[2] Kyoji Moriya,[1] Hideyuki Miyoshi,[1] Hajime Fujie,[1] Yoshizumi Shintani,[1] Hiroshi Yotsuyanagi,[1] Tatsuo Miyamura,[2] Tetsuro Suzuki,[2] and Kazuhiko Koike[1]

The hepatitis C virus (HCV) core protein is involved in viral pathogenesis such as oxidative stress induction and lipid metabolism disturbance, and is primarily located in the cytoplasm and endoplasmic reticulum in association with lipid droplets as well as in the mitochondria. To clarify the impact of the core protein on mitochondria, we analyzed the expression pattern of mitochondrial proteins in core protein-expressing cells by two-dimensional polyacrylamide gel electrophoresis. Several proteins related to the mitochondrial respiratory chain or protein chaperons were identified by mass spectrometry. Among the identified proteins with consistently different expressions, prohibitin, a mitochondrial protein chaperon, was up-regulated not only in core-expressing cells but also in full-genomic replicon cells and livers of core-gene transgenic mice. The stability of prohibitin was increased through interaction with the core protein. Further analysis demonstrated that interaction of prohibitin with mitochondrial DNA-encoded subunits of cytochrome c oxidase (COX) was disturbed by the core protein, resulting in a significant decrease in COX activity. *Conclusion:* The HCV core protein affects the steady-state levels of a subset of mitochondrial proteins including prohibitin, which may lead to an impaired function of the mitochondrial respiratory chain with the overproduction of oxidative stress. (HEPATOLOGY 2009;50:378-386.)

The hepatitis C virus (HCV) is a causative agent of chronic hepatitis, which often leads to cirrhosis and, eventually, to the development of hepatocellular carcinoma (HCC). However, the mechanism of hepatocarcinogenesis in HCV infection is not yet fully elucidated. The HCV core protein forms the viral nucleocapsid protein and has various properties that modulate cellular processes in numerous ways. The core protein binds to cellular proteins, suppresses or enhances apoptosis, and modulates the transcription of some host genes.[1] In addition, transgenic mice expressing the core protein develop HCC,[2-4] indicating a direct contribution of the core protein to the pathogenesis of hepatitis C.

The core protein is mostly localized to the endoplasmic reticulum (ER), but we and other groups have shown its localization to the mitochondria in cultured cells and transgenic mice.[2,5,6] In addition, the double structure of mitochondrial membranes is disrupted in hepatocytes of core-gene transgenic mice.[2-4] Evidence suggests that the core protein modulates some mitochondrial functions, including fatty acid β-oxidation, the impairment of which may induce lipid abnormalities and hepatic steatosis. In addition, the mitochondrion is an important source of reactive oxygen species (ROS). In livers of transgenic

Abbreviations: 2D-PAGE, two-dimensional polyacrylamide gel electrophoresis; COX, cytochrome c oxidase; ER, endoplasmic reticulum; Ero1, ER protein endoplasmic oxidoreduction-1; HCC, hepatocellular carcinoma; HCV, hepatitis C virus; HSP, heat shock protein; IFN, interferon; MnSOD, manganese superoxide dismutase; NS, nonstructural; OST48, oligosaccharyltransferases-48; PDH, pyruvate dehydrogenase; PDI, protein disulfide isomerase; ROS, reactive oxygen species; TFA, trifluoroacetic acid.

From the [1]Department of Internal Medicine, Graduate School of Medicine, University of Tokyo; [2]Department of Virology II, National Institute of Infectious Diseases, Tokyo, Japan.

Received June 17, 2008; accepted March 20, 2009.

Supported by a grant-in-aid for Scientific Research from the Japan Society for the Promotion of Science, from the Ministry of Health, Labour and Welfare of Japan (Research on Hepatitis), from the Ministry of Education, Culture, Sports, Science and Technology (Priority Area), from The Sankyo Foundation of Life Science, and from The Charitable Trust Araki Memorial Promotion Fund. T.T. is an awardee of the Research Resident Fellowship from the Viral Hepatitis Research Foundation of Japan.

Address reprint requests to: Kazuhiko Koike, M.D., Ph.D., Department of Gastroenterology, Internal Medicine, Graduate School of Medicine, University of Tokyo, 7-3-1 Hongo, Bunkyo-ku, Tokyo 113-8655, Japan. E-mail: kkoike-tky@umin.ac.jp; fax: (81) 3-5800-8799

Published online in Wiley InterScience (www.interscience.wiley.com).

DOI 10.1002/hep.22998

Potential conflict of interest: Nothing to report.

Additional Supporting Information may be found in the online version of this article.

mice harboring the core gene, increased ROS production has been observed.[7-9] A recent study found, by the proteomic profiling of biopsy specimens, that an impairment in key mitochondrial processes, including fatty acid oxidation and oxidative phosphorylation, and in the response to oxidative stress occurs in HCV-infected human liver with advanced fibrosis.[10] Therefore, it is probable that the HCV core protein affects mitochondrial functions because such pathogenesis is observed in both HCV core-transgenic mice and HCV-infected patients.[11-13]

The recent progress in proteomics has opened new avenues for disease-related biomarker discovery. Among proteomics approaches, two-dimensional polyacrylamide gel electrophoresis (2D-PAGE) is a technique for the separation and identification of proteins in a sample by displacement in two dimensions oriented at right angles to one another. This method is generally used as a component of proteomics and is the step used for the isolation of proteins for further characterization by mass spectrometry. 2D-PAGE is particularly useful when comparing two related samples such as healthy and diseased tissue. For example, proteins that are more abundant in diseased tissue may represent novel drug targets or diagnostic markers. In fact, several candidate biomarkers for many human cancers have been identified by this approach.[14] There are, however, tens of thousands of proteins in a cell, differing in abundance over six orders of magnitude. 2D-PAGE is not sensitive enough to detect rare proteins, and hence many proteins are not resolved. Therefore, splitting a sample into different fractions is often necessary to reduce the complexity of protein mixtures prior to 2D-PAGE. For this advantage, Lescuyer et al.[15] performed a 2D-PAGE of human mitochondrial proteins derived from the placenta and identified proteins mainly by peptide mass fingerprinting.

In this study, we performed a 2D-PAGE of mitochondria isolated from HepG2 cells stably expressing the HCV core protein and identified several proteins of different expressions when compared with control HepG2 cells. Among up-regulated proteins in the core-expressing cells, we focused on prohibitin, which functions as a mitochondrial protein chaperon, and found that the core protein interacts with prohibitin and represses the interaction between prohibitin and subunit proteins of cytochrome c oxidase (COX), which may lead to decreases in the expression level of the proteins and in COX activity. These results may explain the pathogenesis of liver disease in HCV infection including ROS induction.

Materials and Methods

Cells and Purification of Mitochondria. Hep39 cells,[16] which stably express the HCV core protein, and control HepG2 cells (Hepswx) were grown in Dulbecco's modified Eagle medium (DMEM) containing 10% fetal bovine serum and 1 mg/mL G418. Mitochondria were purified using Nycodenz (Nycomed Pharma, Zürich, Switzerland) according to the protocols reported by Okado-Matsumoto et al.[17] For transient transfection experiments, HepG2 cells were transfected with a core-expression plasmid using TransIT-LT1 (Mirus Bio, Madison, WI). Huh7 cells harboring HCV genotype 1b full-genomic (RCYM1)[18] or subgenomic replicon (5-15), and livers of 3-month-old core-gene transgenic mice[2] were also used for the analysis.

2D-PAGE. Gel electrophoresis in the first dimension was performed using an immobilized pH gradient gel (Immobiline Dry Strip gel, pH 4-7 linear, 13 cm; GE Healthcare, Uppsala, Sweden). The two-dimensional separation was performed on 12.5%, 14 × 16 cm^2, SDS polyacrylamide gels. After the electrophoresis, gels were silver-stained using a silver staining kit (GE Healthcare) according to the manufacturer's protocols. The stained gels were scanned and electronic images of the gels were analyzed using ImageMaster 2D Elite software (GE Healthcare).

In-Gel Digestion and Matrix-Assisted Laser Desorption Ionization, Time-of-Flight Mass Spectrometry (MALDI-TOF-MS). Protein spots on the gels were excised and a "control" piece was cut from a blank region of the gel and processed in parallel with the sample. In-gel digestion with trypsin was performed as reported.[19] The resulting peptides were concentrated using Zip-Tip C18 (Millipore, Bedford, MA). The peptide mixtures were eluted from Zip-Tip with 75% acetonitrile in 0.1% trifluoroacetic acid (TFA). The matrix (α-cyano-4-hydroxycinnamic acid dissolved in 50% acetonitrile, 0.1% TFA) was deposited on a dried sample target. Then 0.5-μL aliquots of the analyte solution were deposited onto matrix surfaces and the solvent was allowed to evaporate at ambient temperature. The digests were analyzed with a TOF mass spectrometer, PE Biosystems Voyager DE STR MALDI (Foster City, CA).

Database Analysis. For protein identification the measured monoisotopic masses of the peptides were analyzed using MS-Fit provided by UCSF (http://prospector.ucsf.edu/ucsfhtml3.2/msfit.htm).

Immunoblotting and Immunoprecipitation. Purified mitochondria were lysed and sonicated in RIPA buffer, then centrifuged at 16,000 rpm for 10 minutes. Protein concentration was determined using a BCA Protein Assay Reagent Kit (Pierce Biotechnology, Rockford, IL). The samples were separated by sodium dodecyl sulfate (SDS)-PAGE and electrotransferred onto a polyvinylidene fluoride membrane (Immobilon; Millipore, Japan), then blocked with BlockAce (Snow Brand, To-

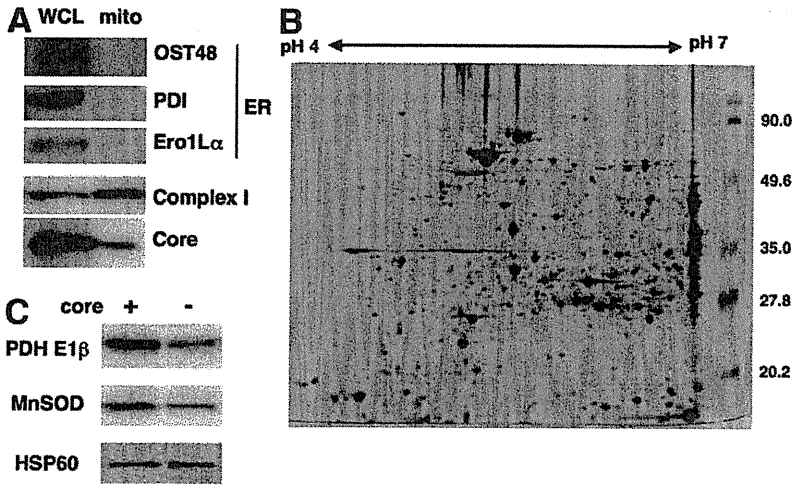

Fig. 1. 2D-PAGE of mitochondria purified from core-expressing cells. (A) Whole-cell lysates (WCL) and purified mitochondria (mito) derived from core-expressing cells were subjected to SDS-PAGE and immunoblotted with anti-core, anti-subunit of complex I (mitochondrial protein), or anti-OST48, PDI, Ero1La (ER proteins) antibodies. (B) Purified mitochondria of core-expressing cells were subjected to 2D-PAGE and the gel was stained with silver. The numbers shown on the right are molecular weights. (C) Purified mitochondria of core-expressing and control cells were subjected to SDS-PAGE and blotted with an anti-E1β subunit of PDH (PDH E1β), anti-MnSOD, or anti-HSP60 antibody.

kyo, Japan). The membrane was subsequently incubated with specific primary antibodies followed by horseradish peroxidase-conjugated secondary antibodies and visualized using SuperSignal West Pico Chemiluminescent Substrate (Pierce). Antibodies against the core protein (Anogen, Mississauga, Canada), manganese superoxide dismutase (MnSOD) (BD Biosciences, San Jose, CA), prohibitin (Neomarkers, Fremont, CA), oligosaccharyltransferase-48 (OST48), heat shock protein (HSP) 60 (Santa-Cruz Biotechnology, Santa Cruz, CA), pyruvate dehydrogenase (PDH), ubiquinol-cytochrome c oxidoreductase, COX (Molecular Probes, Eugene, OR), protein disulfide isomerase (PDI), ER protein endoplasmic oxidoreduction-1 (Ero1)-Lα, and IκBα (Cell Signaling Technology, Danvers, MA), were used as primary antibodies. For immunoprecipitation experiments, cells were lysed in NET-N buffer (20 mM Tris-HCl [pH 8.0], 100 mM NaCl, 1 mM EDTA, 0.5% Nonidet P-40) and the lysates were incubated with anti-prohibitin overnight followed by the addition of protein Sepharose 4B (GE Healthcare), then washed with the same buffer five times. Immunoprecipitates were subjected to SDS-PAGE followed by immunoblotting with specific antibodies.

Determination of COX Activity. COX activity was determined with a MitoProfile Rapid Microplate Assay Kit (MitoSciences, Eugene, OR) using 10 μg of purified mitochondria. The assay was performed three times independently.

Statistical Analysis. Results are expressed as means $\pm$ SE. The significance of the difference in means was determined by Student's t test or Mann-Whitney's U test.

Results

Presence of HCV Core Protein in Purified Mitochondria. Increasing evidence suggests that the HCV core protein is localized to mitochondria as well as to ER and the nucleus. Therefore, we first investigated whether the core protein is expressed in the mitochondria of core-expressing (Hep39) cells used in this study. We used Nycodenz discontinuous gradients to extract mitochondria as described.[17] In the mitochondria derived from core-expressing HepG2 cells, the core protein was detected by immunoblotting, whereas ER resident proteins such as an ER-specific type I transmembrane protein OST48, ER-resident molecular chaperon PDI, and ER membrane-associated N-glycoprotein Ero1-Lα, were not (Fig. 1A). In this fraction, reduced nicotinamide adenine dinucleotide (NADH)-ubiquinone oxidoreductase, complex I of mitochondrial oxidative phosphorylation system, was more strongly expressed than that in the whole cell. These results indicate that the purified mitochondria fraction was free of ER, and that a portion of the core protein was localized to the mitochondria in core-expressing cells.

Proteomics Analysis of Mitochondria by 2D-PAGE. For proteomics analysis, purified mitochondrial proteins derived from core-expressing cells were subjected to 2D-PAGE followed by silver-staining of the gel. In this study we analyzed only acidic proteins using IPG strips covering pH 4 to pH 7 because the analysis of acidic proteins by 2D-PAGE is relatively easy. The mitochondrial fraction was also extracted from Hepswx, a control cell line resistant to G418 but does not express the core protein, then similarly subjected to 2D-PAGE and used for comparing the expression pattern. We repeated the above procedure (purification of mitochondria, 2D-PAGE, and silver-staining) five times, and confirmed a similar expression pattern in core-expressing cells. The representative gel image is shown in Fig. 1B. ImageMaster 2D Elite software detected about 1100 spots on the silver-stained acidic gel, i.e., at pH 4-7 and Mrs of 20-100 kDa. The number of

Table 1. Proteins of Differential Expression in Mitochondria of Core-Expressing Cells

Protein Name	Fold Change (Mean ± SD)
Increased	
Succinyl-CoA:ketoacid CoA transferase	10.43 ± 1.29
NADH-specific isocitrate dehydrogenase a subunit precursor	9.64 ± 4.66
Unknown	8.65 ± 2.40
GrpE-like protein co-chaperon	5.71 ± 0.49
Leucine aminopeptidase	4.26 ± 1.14
Pyruvate dehydrogenase E1 component b subunit	3.79 ± 1.34
CG015alt2	3.18 ± 0.80
HSP70	3.11 ± 1.39
Prohibitin	2.60 ± 0.24
3-Hydroxyisobutyrate dehydrogenase	2.47 ± 0.77
HSPC108	2.46 ± 0.69
MnSOD	2.35 ± 0.65
Ubiquinol-cytochrome c oxidoreductase core I protein	2.00 ± 0.23
Decreased	
Aldehyde dehydrogenase 2	0.12 ± 0.02
Aldehyde dehydrogenase 5 precursor	0.25 ± 0.03
ATP synthase a subunit isoform 1	0.50 ± 0.09
Reference protein	
HSP60	1.02 ± 0.02

protein spots was smaller than those reported in a recent study investigating the human placental mitochondrial proteome.[15]

We then compared the intensity of the spots between core-expressing and control cells. Analysis of repeated experiments by Student's t test revealed 13 increased and three decreased spots in intensity in core-expressing cells. These spots were excised and digested with trypsin, then proteins were identified by mass spectrometry. The names of the identified proteins are listed in Table 1. Among them were proteins related to mitochondrial respiratory chain, protein chaperons, and lipid metabolism. Because antibodies to some of these proteins are commercially available, expression levels of the proteins were examined by immunoblotting. The expression levels of the PDH-E1β subunit and MnSOD, which were identified as increased proteins, were higher in core-expressing cells than in control cells (Fig. 1C), whereas that of HSP60, which was identified as having a similar expression, was unchanged.

Up-regulation of Prohibitin by the Core Protein. Among the identified proteins, we focused on prohibitin, an up-regulated protein in mitochondria of core-expressing cells (Fig. 2A). Prohibitin is a mitochondrial protein associated with cell proliferation.[20] It also works as a chaperon of mitochondrial proteins.[21,22] We confirmed an increased prohibitin expression level in core-expressing cells

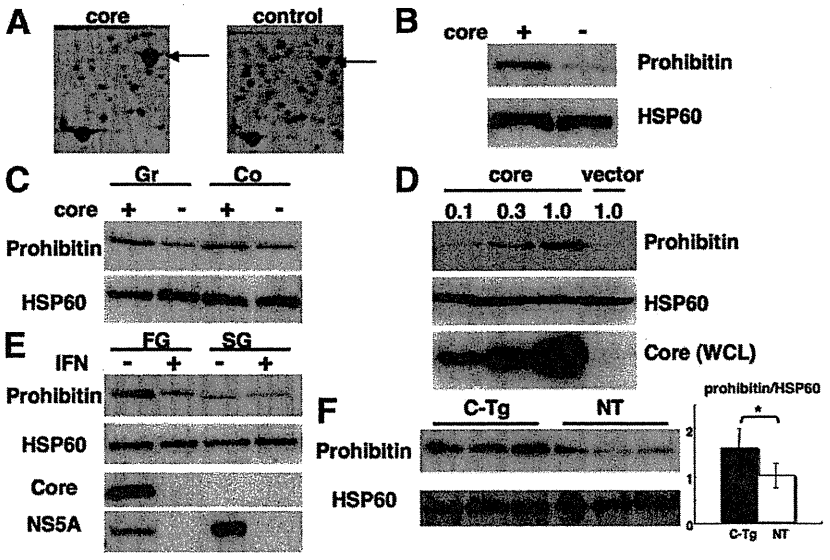

Fig. 2. Up-regulation of prohibitin in core-expressing cells. (A) Protein spot corresponding to prohibitin (arrow) in 2D-PAGE. (B) Purified mitochondria from core-expressing or control cells were subjected to SDS-PAGE and immunoblotted with anti-prohibitin or anti-HSP60 antibody. (C) Mitochondria were purified from growing (Gr) or confluent (Co) cells in 100-mm dishes and subjected to SDS-PAGE, then immunoblotted with an anti-prohibitin or anti-HSP60 antibody. (D) HepG2 cells in six-well plates were transfected with different amounts (μg) of core-expressing plasmid and mitochondrial proteins were analyzed by immunoblotting with anti-prohibitin or anti-HSP60 antibody. The expression levels of the core protein in whole-cell lysates (WCL) were also determined. (E) Cells harboring HCV replicon were untreated or treated with IFN and expression levels of prohibitin in mitochondria were determined. Expression of HCV core and NS5A proteins was also examined. FG, full-genomic replicon cells; SG, subgenomic replicon cells. (F) Expression levels of prohibitin in mitochondria were determined in liver tissues HCV core-gene transgenic and nontransgenic mice. Prohibitin/HSP60 expression levels were determined by densitometry. C-Tg, core-gene transgenic mouse; NT, nontransgenic littermate (n = 3) *$P < 0.05$.

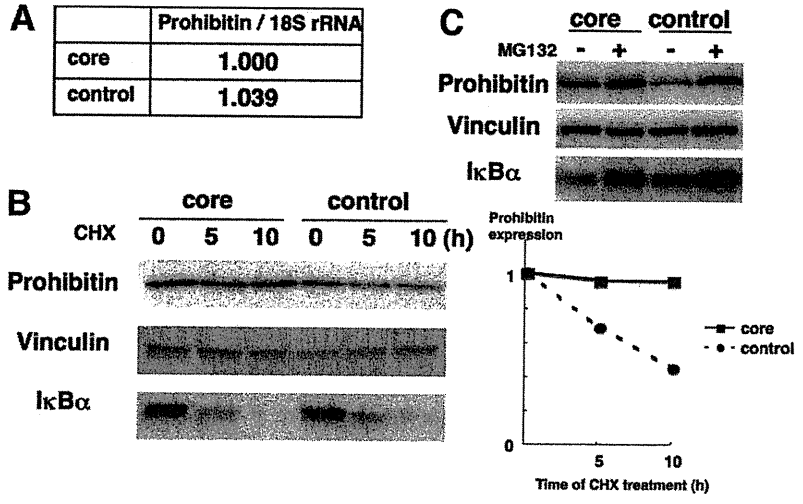

Fig. 3. Increased protein stability of prohibitin in core-expressing cells. (A) RNA was extracted from core-expressing and control cells, and the amount of specific mRNA was determined by real-time PCR with specific primers/probe against prohibitin. The amount of prohibitin mRNA was standardized by that of 18S ribosomal RNA (18S rRNA). (B) Cells were incubated with 100 ng/mL cycloheximide and harvested at the timepoints indicated above the lanes (numbers are hours of cycloheximide treatment). Whole-cell lysates were subjected to SDS-PAGE and immunoblotted with anti-prohibitin, anti-IκBα, or anti-vinculin (as an internal standard) antibody. The intensity of each band was measured by densitometry, and expression levels (prohibitin/vinculin) are shown in the right panel. (C) Cells were harvested after incubation with 20 μM MG132 for 8 hours and subjected to immunoblotting with anti-prohibitin, anti-IκBα, or anti-vinculin antibody.

by immunoblotting (Fig. 2B). Because prohibitin is associated with cell proliferation, it is possible that prohibitin expression changed according to the cell proliferative status. As shown in Fig. 2C, core-expressing cells had high prohibitin expression levels in the cells in both confluent growth and growing statuses compared with control cells. We also determined the expression levels in cells synchronized with aphidicolin followed by l-mimosine treatment and found an increased expression level in core-expressing cells (data not shown). To exclude the possibility that the increased prohibitin expression level is due to the expansion of limited cell clones, not specific to the core protein expression, we examined prohibitin expression in cells transiently expressing the core protein and found that prohibitin expression level increased dose-dependently in core-expressing cells (Fig. 2D). We also examined the prohibitin expression levels in Huh7 cells harboring full- or subgenomic HCV replicon. For this purpose, we used interferon (IFN)-treated replicon cells (cured cells) as a control. Core and nonstructural (NS)5A proteins were not detected after treatment of full-genomic replicon cells with IFN, suggesting a successful elimination of replicon. Prohibitin expression levels in cells with full-genomic replicon were increased compared with those in IFN-treated cured cells, whereas levels of prohibitin expression were low in subgenomic replicon cells regardless of IFN-treatment (Fig. 2E). In addition, prohibitin expression levels were also increased in livers of 3-month-old transgenic mice expressing the core protein compared with those in nontransgenic littermates (Fig. 2F).

We next sought to determine the mechanism of the increased steady-state level of prohibitin in core-expressing cells. To determine prohibitin messenger RNA (mRNA) expression, we performed a real-time polymerase chain reaction (PCR) using specific primers/probe. No difference in prohibitin mRNA was observed between core-expressing and control cells (Fig. 3A). We next determined the stability of prohibitin in these cells. By treating the cells with cycloheximide, the expression levels of prohibitin gradually decreased in control cells (Fig. 3B). On the other hand, in core-expressing cells prohibitin was hardly degraded by cycloheximide treatment for 10 hours, whereas IκBα was equally degraded in both cells. This result suggests that prohibitin was stabilized in the presence of the core protein. Because prohibitin has been shown to be degraded by proteasome,[23] we examined expression levels of prohibitin in the presence of proteasome inhibitor MG132. By treatment with MG132, prohibitin expression was increased to the similar level in core-expressing and control cells. These results suggest that the core protein may inhibit proteasomal degradation of prohibitin by some mechanism, including the prevention of degradation by interaction with the core protein. Then, core-expressing cells were lysed and subjected to immunoprecipitation with an anti-prohibitin antibody. As shown in Fig. 4, the core protein was coimmunoprecipitated with an anti-prohibitin antibody. To exclude a nonspecific interaction with the antibody or Sepharose beads, cells expressing a small amount of prohibitin by transfection with small interfering RNA (siRNA) against prohibitin were also examined. In these cells the amount of the coimmunoprecipitated core protein decreased. In addition, the core protein was not coimmunoprecipitated by control immunoglobulin G (IgG), indicating a specific interaction of prohibitin with the core protein. These results suggest that prohibitin expression increased in core-expressing cells owing to the increased stability presumably by interaction with the core protein.

Impaired Chaperon Function of Prohibitin in Core-Expressing Cells. We next examined the effect of

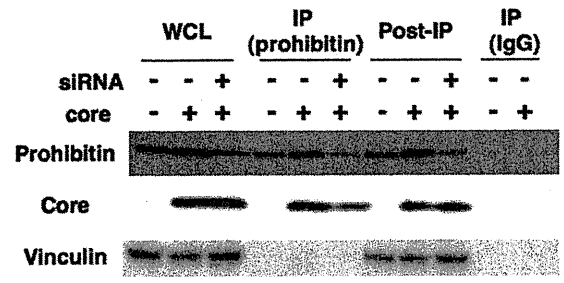

Fig. 4. Interaction of the core protein with prohibitin. Core-expressing and control cells were transfected with or without siRNA against the prohibitin gene, then harvested and lysed in NET-N buffer 3 days after transfection. Whole-cell lysates (WCL) were immunoprecipitated (IP) with an anti-prohibitin antibody or control IgG and immunoblotted with anti-prohibitin or anti-core antibody. Supernatants after the immunoprecipitation were harvested and similarly immunoblotted (Post-IP).

the interaction of prohibitin with the core protein on the function of prohibitin. Prohibitin works as a chaperon of mitochondrial proteins. Nijtmans et al.[21] demonstrated that prohibitin exerts a chaperon function particularly for the stabilization of mitochondrial DNA-encoded proteins. COX is a mitochondrial respiratory complex IV formed by 14 subunits, 10 of which are encoded by nuclear DNA and the rest by mitochondrial DNA.[24] We examined the interaction of prohibitin with subunit II of COX encoded by mitochondrial DNA. As shown in Fig. 5A, the level of COX II coimmunoprecipitated with an anti-prohibitin antibody was decreased in core-expressing cells, although the amount of immunoprecipitated prohibitin was higher than that in control cells. On the other hand, the subunit IV of COX encoded by nuclear DNA was similarly coimmunoprecipitated between core-expressing and control cells. When prohibitin expression was decreased by siRNA transfection, coimmunoprecipitation of COX subunits was similarly decreased with the amount of immunoprecipitation of prohibitin itself being low. We next determined expression levels of COX subunits in the mitochondria in these cells. Expression levels of mitochondrial DNA-encoded subunits I and II in core-expressing cells were decreased, whereas the levels of nuclear DNA-encoded subunits IV and VIb were similar to those in control cells. When transfected with prohibitin-siRNA, expression levels of all of the COX subunits examined were decreased in both core-expressing and control cells, suggesting that protein levels of these subunits are dependent on prohibitin (Fig. 5B, see Supporting Fig. 1 for densitometry). Similar data were observed when blots for COX II and IV were developed together in the same membrane (Supporting Fig. 2). We also determined COX activity in these cells and found that core-expressing cells had a significantly decreased COX activity (about 70% of that in control cells, Fig. 5C). These results suggest that interaction of prohibitin with the core protein is associated with an impaired function of prohibitin as a mitochondrial chaperon, which may trigger disordered assembly and function of mitochondrial respiratory complexes.

Discussion

In the present study we analyzed expression levels of mitochondrial proteins in HepG2 cells expressing the HCV core protein and identified a set of proteins with different expressions. Some of those proteins were related to the mitochondrial respiratory chain (Table 1). Because the core protein was shown to be associated with the induction of oxidative stress,[7-9] the core protein may modulate the expression and function of proteins forming mitochondrial respiratory complexes, which naturally

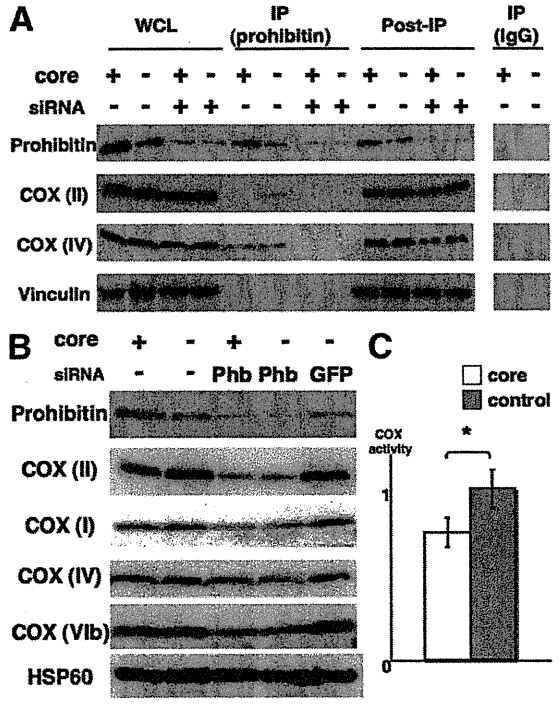

Fig. 5. Effects of core-prohibitin interaction on interaction/expression of COX subunit proteins and COX activity. (A) Whole-cell lysates (WCL) of core-expressing and control cells were subjected to immunoprecipitation with an anti-prohibitin antibody or control IgG, and the interaction of prohibitin with COX subunits was determined by immunoblotting of immunoprecipitated proteins (IP). Supernatants after the immunoprecipitation were harvested and similarly immunoblotted (Post-IP). (B) Cells were transfected with or without siRNA against the prohibitin (Phb) or GFP gene and harvested 3 days after transfection for purification of mitochondria. Purified mitochondria were subjected to SDS-PAGE and immunoblotted with several anti-COX subunits antibodies. The expression levels of HSP60 were also examined as an internal control. (C) COX activity was determined by measuring cytochrome c oxidation. The activity was normalized by taking the average rate of control cells as 1. Data shown are means ± SE (n = 5). *$P < 0.05$.

leads to ROS accumulation. In addition, MnSOD, which plays a key role in protecting cells from oxidative damage, was up-regulated in core-expressing cells, reflecting ROS increase in the cells. Several protein chaperons such as HSP70 and GrpE-like protein co-chaperon were also identified as up-regulated proteins. Because these proteins are known to be important in the mitochondrial protein-import mechanisms, the modulated expression of these proteins may be associated with the different expressions of the identified mitochondrial proteins.

Prohibitin, a mitochondrial protein chaperon, was identified as an up-regulated protein in core-expressing cells. Prohibitin is a ubiquitously expressed and highly conserved protein that was originally determined to play a predominant role in inhibiting cell-cycle progression and cellular proliferation by attenuating DNA synthesis.[20,25] Prohibitin is present in the nucleus and interacts with transcription factors that are important in cell cycle progression. In core-expressing cells used in this study, prohibitin was also detected in the nucleus and its expression level was also higher than that in control Hepswx cells or HepG2 cells (data not shown). The growth rate of core-expressing cells, however, was similar to that of control cells (data not shown). The physiological significance of the high expression level of prohibitin in the nucleus remains to be determined, but it may be related to enhanced apoptosis by Fas ligand, as shown by Ruggieri et al.,[16] because prohibitin interacts with E2F, Rb, and p53 and modulates the transcription activity of these factors and induces apoptosis.[26,27]

Mitochondrial prohibitin acts as a protein chaperon by stabilizing newly synthesized mitochondrial translation products through direct interaction.[21] We examined the interaction between prohibitin and mitochondrially encoded subunit II of COX and found a suppressed interaction between these proteins in core-expressing cells. In addition, there are several studies that showed the association of prohibitin with the assembly of mitochondrial respiratory complex I as well as complex IV (COX).[21,28] Complex I also consists of both nuclear- and mitochondrial-DNA-encoded subunits; therefore, it is probable that the assembly and function of complex I are impaired by the core protein. We attempted to examine the interaction of prohibitin with the mitochondrial DNA-encoded subunit of complex I, but commercially available antibodies against this subunit could not detect the protein itself by immunoblotting (data not shown). With respect to the complex I function, we found a decreased complex I activity in core-expressing cells (H. Miyoshi et al., manuscript in preparation). Other groups have also shown that complex I activity is decreased in the liver of transgenic mice harboring HCV core and envelope genes[9] as well as in cultured cells.[29] From these findings, the interaction between prohibitin and the core protein may impair the function of complex I as well as complex IV, leading to an increase in ROS production. In fact, the suppression of the prohibitin function is shown to result in an increased production of ROS,[30] a phenomenon observed in core-expressing cells used in this study (Miyoshi et al., in prep.) as well as in the liver of core-gene transgenic mice.[7,8] Interestingly, Berger and Yaffe[31] showed that loss of function of prohibitin leads to an altered mitochondrial morphology, that is, the loss of the normal reticular morphology and organized mitochondrial distribution. In hepatocytes from the core-gene transgenic mice, we observed a change in morphology of mitochondria, a disappearance of the double structure of mitochondrial membranes.[2] These changes in mitochondrial morphology are somewhat different, but the dysfunction of prohibitin may be responsible for the morphological abnormality of mitochondria observed in the core-gene transgenic mice.

We concluded that prohibitin overexpression is due to increased stability induced by the interaction with the core protein. In this study we showed that prohibitin might be degraded by proteasome, although we could not detect ubiquitinated forms of prohibitin. If the degradation is mediated by ubiquitin as reported,[23] it is possible that the interaction with the core protein interferes with ubiquitin-binding and protects prohibitin from degradation by proteasome. Some posttranslational protein modifications such as phosphorylation are other possible factors for the stabilization, because prohibitin can be serine-phosphorylated[32]; however, in our examination no serine/threonine/tyrosine phosphorylation of prohibitin was detected in core-expressing cells (data not shown). Thus far, there are no studies showing that prohibitin stabilization leads to a suppressed function as a mitochondrial chaperon. Therefore, this finding is novel and noteworthy because the prohibitin expression level has been considered to be proportional to the chaperon function. Prohibitin is highly expressed in several human tumors.[33,34] In addition, a 2D-PAGE of the hepatoma cell line HCC-M identified prohibitin as a positively regulated protein.[35] In these studies, the mechanism of prohibitin overexpression was not elucidated, but considering that prohibitin is associated with the inhibition of cell proliferation, the function of prohibitin is suppressed by stabilization by some molecules in the tumor, similar to the mechanism we suggest in the current study.

In addition to HepG2 cells constitutively expressing the core protein, increased prohibitin expression levels were also found in livers of core-gene transgenic mice.

The difference in expression levels between the transgenic mice and nontransgenic littermates, however, was a little bit smaller than that in the studies of HepG2 cells. This may be due to the low expression level of the core protein in the transgenic mice compared with that in core-expressing HepG2 cells because the expression level of prohibitin was proportionally increased to that of the core protein as shown in this study (Fig. 2D). Otherwise, there might be some *in vivo* mechanism for suppressing prohibitin expression in mice.

In this study, COX subunit IV as well as II were found to interact with prohibitin (Fig. 5A). Although there are no studies demonstrating that prohibitin also works as chaperon for nuclear DNA-encoded mitochondrial proteins as far as we investigated, knockdown of prohibitin expression by siRNA led to decreases in expression levels of both nuclear (COX IV, VIb) and mitochondrial (COX I, II) DNA-encoded subunits in mitochondria (Fig. 5B and Supporting Figs. 1 and 2). We showed that COX IV interacts with prohibitin (Fig. 4), suggesting that prohibitin also works for stable expression of nuclear DNA-encoded COX IV. Degrees of decrease in COX IV and VIb expression, however, were smaller than those in I and II. Prohibitin might contribute to stabilization of COX IV and VIb by mechanism(s) other than chaperon function. Steglich et al.[36] showed that prohibitin regulates protein degradation by the m-AAA protease in mitochondria. Recently, Da Cruz et al.[37] showed that SLP-2, a member of the stomatin gene family, interacts with prohibitin and regulates the expression of mitochondrial proteins such as COX IV and ND6 of complex I encoded by nuclear DNA by AAA proteases. In view of these findings, COX IV and VIb expression in mitochondria is dependent on prohibitin but other factors may also be involved in the attainment of stable expression of these subunits. The expression levels of COX II and IV in the whole-cell lysates were not so drastic among cell samples (Fig. 5A) compared to those in the mitochondria (Fig. 5B). The reason is not clear, but it is possible that redundant proteins such as improperly folded proteins by lack of chaperons were included in the whole-cell lysates.

In summary, we analyzed mitochondrial proteins in core-expressing HepG2 cells by proteomics analysis and identified prohibitin as an up-regulated protein. The dysfunction of prohibitin induced by the core protein may lead to ROS overproduction in the mitochondrion, which plays a key role in the pathogenesis of chronic hepatitis C. The restoration of prohibitin function might be a therapeutic option for correcting the dysregulated assembly and dysfunction of mitochondrial respiratory chain complexes.

Acknowledgment: We thank S. Shinzawa, M. Yahata, and S. Yoshizaki for technical assistance.

References

1. Suzuki R, Suzuki T, Ishii K, Matsuura Y, Miyamura T. Processing and functions of Hepatitis C virus proteins. Intervirology 1999;42:145-152.
2. Moriya K, Fujie H, Shintani Y, Yotsuyanagi H, Tsutsumi T, Ishibashi K, et al. The core protein of hepatitis C virus induces hepatocellular carcinoma in transgenic mice. Nat Med 1998;4:1065-1067.
3. Naas T, Ghorbani M, Alvarez-Maya I, Lapner M, Kothary R, De Repentigny Y, et al. Characterization of liver histopathology in a transgenic mouse model expressing genotype 1a hepatitis C virus core and envelope proteins 1 and 2. J Gen Virol 2005;86:2185-2196.
4. Machida K, Cheng KT, Lai CK, Jeng KS, Sung VM, Lai MM. Hepatitis C virus triggers mitochondrial permeability transition with production of reactive oxygen species, leading to DNA damage and STAT3 activation. J Virol 2006;80:7199-7207.
5. Suzuki R, Sakamoto S, Tsutsumi T, Rikimaru A, Tanaka K, Shimoike T, et al. Molecular determinants for subcellular localization of hepatitis C virus core protein. J Virol 2005;79:1271-1281.
6. Schwer B, Ren S, Pietschmann T, Kartenbeck J, Kaehlcke K, Bartenschlager R, et al. Targeting of hepatitis C virus core protein to mitochondria through a novel C-terminal localization motif. J Virol 2004;78:7958-7968.
7. Moriya K, Nakagawa K, Santa T, Shintani Y, Fujie H, Miyoshi H, et al. Oxidative stress in the absence of inflammation in a mouse model for hepatitis C virus-associated hepatocarcinogenesis. Cancer Res 2001;61:4365-4370.
8. Okuda M, Li K, Beard MR, Showalter LA, Scholle F, Lemon SM, et al. Mitochondrial injury, oxidative stress, and antioxidant gene expression are induced by hepatitis C virus core protein. Gastroenterology 2002;122:366-375.
9. Korenaga M, Wang T, Li Y, Showalter LA, Chan T, Sun J, et al. Hepatitis C virus core protein inhibits mitochondrial electron transport and increases reactive oxygen species (ROS) production. J Biol Chem 2005;280:37481-37488.
10. Diamond DL, Jacobs JM, Paeper B, Proll SC, Gritsenko MA, Carithers RL Jr, et al. Proteomic profiling of human liver biopsies: hepatitis C virus-induced fibrosis and mitochondrial dysfunction. HEPATOLOGY 2007;46:649-657.
11. Moriya K, Yotsuyanagi H, Shintani Y, Fujie H, Ishibashi K, Matsuura Y, et al. Hepatitis C virus core protein induces hepatic steatosis in transgenic mice. J Gen Virol 1997;78(Pt 7):1527-1531.
12. Moriya K, Todoroki T, Tsutsumi T, Fujie H, Shintani Y, Miyoshi H, et al. Increase in the concentration of carbon 18 monounsaturated fatty acids in the liver with hepatitis C: analysis in transgenic mice and humans. Biochem Biophys Res Commun 2001;281:1207-1212.
13. Fujie H, Yotsuyanagi H, Moriya K, Shintani Y, Tsutsumi T, Takayama T, et al. Steatosis and intrahepatic hepatitis C virus in chronic hepatitis. J Med Virol 1999;59:141-145.
14. Cho WC. Contribution of oncoproteomics to cancer biomarker discovery. Mol Cancer 2007;6:25.
15. Lescuyer P, Strub JM, Luche S, Diemer H, Martinez P, Van Dorsselaer A, et al. Progress in the definition of a reference human mitochondrial proteome. Proteomics 2003;3:157-167.
16. Ruggieri A, Harada T, Matsuura Y, Miyamura T. Sensitization to Fas-mediated apoptosis by hepatitis C virus core protein. Virology 1997;229:68-76.
17. Okado-Matsumoto A, Fridovich I. Subcellular distribution of superoxide dismutases (SOD) in rat liver: Cu,Zn-SOD in mitochondria. J Biol Chem 2001;276:38388-38393.
18. Murakami K, Ishii K, Ishihara Y, Yoshizaki S, Tanaka K, Gotoh Y, et al. Production of infectious hepatitis C virus particles in three-dimensional cultures of the cell line carrying the genome-length dicistronic viral RNA of genotype 1b. Virology 2006;351:381-392.

19. Shevchenko A, Wilm M, Vorm O, Mann M. Mass spectrometric sequencing of proteins silver-stained polyacrylamide gels. Anal Chem 1996;68: 850-858.
20. Mishra S, Murphy LC, Murphy LJ. The prohibitins: emerging roles in diverse functions. J Cell Mol Med 2006;10:353-363.
21. Nijtmans LG, de Jong L, Artal Sanz M, Coates PJ, Berden JA, Back JW, et al. Prohibitins act as a membrane-bound chaperone for the stabilization of mitochondrial proteins. EMBO J 2000;19:2444-2451.
22. Back JW, Sanz MA, De Jong L, De Koning LJ, Nijtmans LG, De Koster CG, et al. A structure for the yeast prohibitin complex: structure prediction and evidence from chemical crosslinking and mass spectrometry. Protein Sci 2002;11:2471-2478.
23. Thompson WE, Ramalho-Santos J, Sutovsky P. Ubiquitination of prohibitin in mammalian sperm mitochondria: possible roles in the regulation of mitochondrial inheritance and sperm quality control. Biol Reprod 2003; 69:254-260.
24. Fontanesi F, Soto IC, Horn D, Barrientos A. Assembly of mitochondrial cytochrome c-oxidase, a complicated and highly regulated cellular process. Am J Physiol Cell Physiol 2006;291:C1129-C1147.
25. Mishra S, Murphy LC, Nyomba BL, Murphy LJ. Prohibitin: a potential target for new therapeutics. Trends Mol Med 2005;11:192-197.
26. Fusaro G, Dasgupta P, Rastogi S, Joshi B, Chellappan S. Prohibitin induces the transcriptional activity of p53 and is exported from the nucleus upon apoptotic signaling. J Biol Chem 2003;278:47853-47861.
27. Joshi B, Ko D, Ordonez-Ercan D, Chellappan SP. A putative coiled-coil domain of prohibitin is sufficient to repress E2F1-mediated transcription and induce apoptosis. Biochem Biophys Res Commun 2003;312:459-466.
28. Bourges I, Ramus C, Mousson de Camaret B, Beugnot R, Remacle C, Cardol P, et al. Structural organization of mitochondrial human complex I: role of the ND4 and ND5 mitochondria-encoded subunits and interaction with prohibitin. Biochem J 2004;383:491-499.
29. Piccoli C, Scrima R, Quarato G, D'Aprile A, Ripoli M, Lecce L, et al. Hepatitis C virus protein expression causes calcium-mediated mitochondrial bioenergetic dysfunction and nitro-oxidative stress. HEPATOLOGY 2007;46:58-65.
30. Theiss AL, Idell RD, Srinivasan S, Klapproth JM, Jones DP, Merlin D, et al. Prohibitin protects against oxidative stress in intestinal epithelial cells. FASEB J 2007;21:197-206.
31. Berger KH, Yaffe MP. Prohibitin family members interact genetically with mitochondrial inheritance components in Saccharomyces cerevisiae. Mol Cell Biol 1998;18:4043-4052.
32. Ross JA, Nagy ZS, Kirken RA. The PHB1/2 phosphocomplex is required for mitochondrial homeostasis and survival of human T cells. J Biol Chem 2008;283:4699-4713.
33. Coates PJ, Nenutil R, McGregor A, Picksley SM, Crouch DH, Hall PA, et al. Mammalian prohibitin proteins respond to mitochondrial stress and decrease during cellular senescence. Exp Cell Res 2001;265:262-273.
34. Asamoto M, Cohen SM. Prohibitin gene is overexpressed but not mutated in rat bladder carcinomas and cell lines. Cancer Lett 1994;83:201-207.
35. Seow TK, Ong SE, Liang RC, Ren EC, Chan L, Ou K, et al. Two-dimensional electrophoresis map of the human hepatocellular carcinoma cell line, HCC-M, and identification of the separated proteins by mass spectrometry. Electrophoresis 2000;21:1787-1813.
36. Steglich G, Neupert W, Langer T. Prohibitins regulate membrane protein degradation by the m-AAA protease in mitochondria. Mol Cell Biol 1999; 19:3435-3442.
37. Da Cruz S, Parone PA, Gonzalo P, Bienvenut WV, Tondera D, Jourdain A, et al. SLP-2 interacts with prohibitins in the mitochondrial inner membrane and contributes to their stability. Biochim Biophys Acta 2008;1783: 904-911.